Paleo- and Neo-Tethyan subducted slabs beneath the Eastern Mediterranean region

Douwe J.J. van Hinsbergen[1], Derya Gürer[2], Douwe G. van der Meer[1], Wim Spakman[1]

1. Department of Earth Sciences, Utrecht University, Utrecht, the Netherlands
2. Department of Earth Sciences, Heidelberg University, Heidelberg, Germany

Corresponding author: D.J.J.vanHinsbergen@uu.nl

Abstract

The late Paleozoic to recent Alpine-Himalayan orogen contains the geological remnants of subducted lithosphere of the Paleotethys and Neotethys oceans and of microcontinents within these. Along its ~12,000 km length, this orogenic belt is divided into segments marked by abrupt changes along-strike. These discontinuities align with paleo-transform faults, across which the histories of ocean opening and closure changed, as indicated by plate reconstructions. Here, we test whether seismic tomography revealing slab remnants and corresponding segments in the mantle below the Tethyan realm may be correlated to Paleo- and Neotethyan subduction zones. We focus on the Anatolian segment and its neighboring Aegean and Iranian segments, where deep-mantle slabs were previously not studied in detail. Using a recent, detailed plate tectonic reconstruction placed in a mantle reference frame, to predict where and when slabs were subducted. We then compare these predictions with seismic tomographic images of the mantle beneath the Eastern Mediterranean and Middle Eastern regions. Building on previously interpreted slabs in the Aegean and Iranian region, we identify anomalies of the Anatolian segment. Notably, we identify a sub-horizontal slab between 2200 and 1500 km depth as the remnant of Paleotethyan oceanic lithosphere that subducted between ~240 and 180 Ma. Subsequent Neotethyan subduction generated three major slabs. Two of these (Pontides and Egypt slabs) detached in the late Cretaceous and are now located in the upper part of the lower mantle. The third one (Cyprus slab) resides predominantly in the upper mantle but penetrates the top of the lower mantle where it is overturned, and is still subducting, or possibly detaching, today. The present positions of these slabs likely reflect their past slab detachment locations, whereas their geometries reflect absolute motions (advancing, stationary, or retreating) of their associated paleo-trenches through time. We show that slabs associated with the Aegean, Anatolian, Iranian, and previously identified Tibetan segments define mantle provinces. The transitions between these provinces closely align with the transform-related boundaries that are expressed in orogenic segmentation. Their stability implies minimal paleo-longitudinal mantle flow in the mantle reference frame since the Early Mesozoic. These observations suggests that upper and lower mantle structure is largely explained by near-vertical slab sinking of slabs after their detachment since the Triassic without significant modification by bottom-up-driven, or lateral mantle convective flow.

1. Introduction

The detection of negative and positive seismic wave speed anomalies imaged through global seismic mantle tomography revolutionized Earth sciences by providing a first 'geological', or geophysical, map of Earth's heterogenous mantle (Becker and Boschi, 2002, Bijwaard *et al.*, 1998, Fukao *et al.*, 2001, Grand *et al.*, 1997, Van der Hilst *et al.*, 2007, Van der Voo *et al.*, 1999a, b). Seismically slower and likely hotter, columnar features have been correlated to mantle plumes (Goes *et al.*, 1999, Nolet *et al.*, 2007, Bijwaard and Spakman,

2

1999, French and Romanowicz, 2015), whereas seismically faster regions are thought to be colder than the ambient mantle and were shown to correlate with subducting slabs in the upper as well as the lower mantle (Grand *et al.*, 1997, Van der Voo *et al.*, 1999a, b, Hafkenscheid *et al.*, 2006, van der Meer *et al.*, 2010, 2018, Parsons *et al.*, 2020, Qayyum *et al.*, 2022, Wu *et al.*, 2016, Sigloch and Mihalynuk, 2013). These slab remnants provide unique markers for reconstructing part of the evolution of the mantle, and place constraints on the kinematics of mantle flow operating over geological timescales within Earth's interior.

Subducted slabs leave distinct geological records at the surface in the form of accretionary orogens and associated arcs (e.g., Cawood *et al.*, 2009, van Hinsbergen and Schouten, 2021). Systematic correlations between such orogenic records and slabs under the assumption that deeper slabs tend to be older (van Hinsbergen *et al.*, 2005, Hafkenscheid *et al.*, 2006, van der Meer *et al.*, 2010, 2018, Butterworth *et al.*, 2014), revealed depth-dependent first-order slab sinking rates of 0.5-1.5 cm/yr, varying with depth in the lower mantle (van der Meer *et al.*, 2018). The deepest tomographic anomalies, near the core-mantle boundary, correlate to lithosphere that subducted around ~250 Ma (van der Meer *et al.*, 2018). Those correlations were largely based on relatively isolated subduction systems, because for complexly stacked slabs the tectonic evolution and spatial extents in seismic wave tomographic models are more ambiguous to unravel. However, linking the subduction history of the Tethyan oceans, which culminated in the formation of the Alpine-Himalayan orogenic belt, is less straightforward. There, opening and subduction of oceanic basins and collisions of microcontinents occurred since the late Paleozoic, and the arrest of one subduction system often formed the prelude of formation of the next (Wan *et al.*, 2019, Ma *et al.*, 2025) - even multiple subduction systems may have been active at the same time (Jagoutz *et al.*, 2015, Gürer *et al.*, 2022). Moreover, Tethyan trenches were often mobile, advancing, retreating, or even moving trench-parallel (Jagoutz *et al.*, 2015, Jolivet *et al.*, 2015, Parsons *et al.*, 2021) which must have deformed slabs and dragged them through the mantle (Spakman *et al.*, 2018, Sigloch and Mihalynuk, 2013, Qayyum *et al.*, 2022, Chen *et al.*, 2024, Fuston *et al.*, 2025). Interpreting such stacked and deformed Tethyan slab systems, as those reconstructed for the opening and closure histories of the Tethyan ocean basins that ultimately led to the formation of the Tibetan Plateau and Himalaya since the Triassic remains challenging (Parsons *et al.*, 2020, Qayyum *et al.*, 2022, Van der Voo *et al.*, 1999b, Hafkenscheid *et al.*, 2006). Doing so requires integration of surface kinematic history of trenches with modern, complex mantle structure.

The Alpine-Himalayan orogenic belt is segmented by abrupt along-strike changes, which, according to plate tectonic reconstructions, coincide with paleo-transform faults across which oceanic opening and subduction histories changed (Stampfli and Borel, 2002, Lom and van Hinsbergen, 2026, van Hinsbergen *et al.*, 2026, Tapponnier *et al.*, 1986, Handy *et al.*, 2010, Zahirovic *et al.*, 2016) (Figure 1). Seismic tomographic images below the Tethyan realm also show abrupt changes in upper and lower mantle structure which have previously been correlated to these segments (e.g., Hafkenscheid *et al.*, 2006, van der Meer *et al.*, 2010, Handy *et al.*, 2010), and detailed interpretations of Tethyan subducted slabs have been proposed for the

Figure 1. Plate tectonic reconstruction of the Tethyan oceans at 190 Ma, illustrating the transform-bounded plate tectonic segmentation of the oceanic plate system. Based on the Utrecht Paleogeographic Model as summarized in van Hinsbergen et al. (2026) with plate tectonic interpretations as in Lom and van Hinsbergen (2026). EMO = Eastern Mediterranean Ocean.

Tibetan (Parsons *et al.*, 2020, Qayyum *et al.*, 2022, Replumaz *et al.*, 2004, 2010a), Iranian (van der Meer *et al.*, 2010, 2018, Agard *et al.*, 2011), and Balkan segments (Maffione and van Hinsbergen, 2018, Handy *et al.*, 2010). However, for the Anatolian segment, which kinematically may be the most complex of the four regions (Figure 1), only few of the mantle tomographic anomalies have been interpreted (van der Meer *et al.*, 2010), mostly limited to upper mantle structure (Biryol *et al.*, 2011, Confal *et al.*, 2025). Recent detailed restorations of eastern Mediterranean tectonic evolution since the Triassic (van Hinsbergen *et al.*, 2020, 2024) now invites an attempt at interpreting upper and lower mantle structure below this region in terms of Paleo- and Neotethyan slabs.

We first review the first-order plate tectonic evolution of Paleo- and Neotethys closure, highlighting the subduction zones and their motions that are key to interpreting present-day mantle structure. Next, we provide an overview of modern mantle structure, both in map and in cross-section, and identify tomographic anomalies and their interpretations as slab remnants. Subsequently, we interpret the tomography from top to bottom, and geologically from young to old, to assess which of the identified positive wave speed

tomographic anomalies may represent subducted Neotethyan and Paleotethyan lithosphere. Based on this analysis, we evaluate whether the Tethyan segments reconstructed from west to east may be recognized in modern mantle structure, and we discuss the implications of our findings for mantle kinematics and dynamics.

2. Tectonic evolution of the Tethyan oceans

2.1 Synopsis of Tethys-wide evolution

The history of the Tethyan oceans is an interpretation that derived from tectonic reconstructions of the Alpine-Himalayan mountain belt (Stöcklin, 1974, Şengör, 1979), the W-E striking orogenic belt that extends from the Mediterranean region to SE Asia. Its geology consists of continent-derived, accreted crustal units incorporated into fold-and-thrust belts, separated from the major continents of Eurasia, Africa, Arabia, and India by suture zones that become younger from north to south. These suture zones contain the remnants of oceanic lithosphere and associated sediments, providing key evidence of past ocean basins, collectively referred to as the Tethyan oceans. The Paleotethys and Neotethys oceans once separated Gondwana (Africa, Arabia, India, Australia) from proto-Eurasia during the late Paleozoic to Triassic assembly of the supercontinent Pangea (e.g., Şengör, 1984)). Plate reconstructions that restore the opening of the Atlantic and Indian oceans indicate that the Tethys ocean was triangular and widened eastward (Figure 1). Following the break-up of Pangea and the opening of the Atlantic and Indian Oceans since the Jurassic, the various Tethyan ocean basins progressively closed, producing the modern Alpine-Himalayan orogenic belt.

The opening and closure of the Tethyan oceans must have been plate tectonically complex. First, the series of mostly E-W trending suture zones and intervening continental fragments preserved in the Tethys-derived orogens reveal an across-strike segmentation within the Tethyan domain, that likely reflect transform faults that played a role during the opening and closure of multiple Tethyan ocean basins - analogous to modern Atlantic Ocean that hosts multiple oceanic basins that linked up (e.g., Torsvik *et al.*, 2009, Labails *et al.*, 2010). These transforms were then inherited in the subsequent orogenic architecture and evolution (Barrier and Vrielynck, 2008, van Hinsbergen *et al.*, 2020). The Paleozoic 'Paleotethys' ocean closed during Permian to Jurassic time (with ages varying along-strike), well before the final Cenozoic collisions of the major Tethys-bounding continents (Şengör, 1984, Stampfli and Borel, 2002). These early collisions were facilitated by the opening of new oceanic basins along the northern margin of Gondwana, which detached the 'Cimmerian' continental fragments from the latter, transporting these towards the southern margin of Eurasia (Şengör, 1984, Şengör *et al.*, 2023) (Figure 1).

The opening and closure of these oceans was not uniform along the Tethys but was instead segmented by major along-strike oceanic transform faults (Lom and van Hinsbergen, 2026, van Hinsbergen

et al., 2020, Handy *et al.*, 2010, Zahirovic *et al.*, 2016, Stampfli and Borel, 2002) into what we refer to here the Balkan, Anatolian, Iranian, and Tibetan segments (Figure 1). The Tibetan segment had the most 'Tethyan' basins because multiple post-Paleotethyan continental fragments broke off Gondwana, opening and closing oceans, and colliding (Yin and Harrison, 2000, Wan *et al.*, 2019, Kapp and DeCelles, 2019, van Hinsbergen *et al.*, 2012). In the Iranian segment, closure of the Paleotethys in late Permian and Triassic time was associated with opening of a single Neotethys Ocean that closed until the late Oligocene (Lom and van Hinsbergen, 2026, Stampfli and Borel, 2002, Muttoni *et al.*, 2009). In the Anatolian and Balkan segments, Paleotethys closure and Neotethys opening occurred later, in late Triassic to middle Jurassic times (Şengör and Yilmaz, 1981, van Hinsbergen *et al.*, 2020, Dokuz *et al.*, 2017). Moreover, the southern margin of the Neotethys was formed by an extended microcontinental region, Greater Adria, that itself separated from Africa by the Eastern Mediterranean Ocean in Triassic to Jurassic time (Speranza *et al.*, 2012) (Figure 1).

The along-strike and across-strike segmentation, closure of the ocean basins was not always accommodated at only 'Andean' style subduction zones along continental margins, but also at intra-oceanic subduction zones and backarc basins. Intra-oceanic subduction zones formed at extinct mid-ocean ridges, parallel to passive margins, but also along the segment-bounding transforms within the Neotethys Ocean (van Hinsbergen *et al.*, 2021, Maffione and van Hinsbergen, 2018). This configuration led to widespread ophiolite emplacement upon arrival of Tethyan continental margins in these intra-oceanic subduction zones (e.g., Robertson, 2002). Collectively, the along- and across-strike segmentation of ocean basins and the closure of these oceans at multiple, sometimes parallel subduction systems with segments that underwent separate histories of trench motion explains the complex and laterally discontinuous collection of tomographic positive wavespeed anomalies interpreted as slabs in the mantle below the former Tethyan region (Van der Voo *et al.*, 1999b, Parsons *et al.*, 2020, Qayyum *et al.*, 2022, van der Meer *et al.*, 2010, 2018, Hafkenscheid *et al.*, 2006, Replumaz *et al.*, 2004, Boutoux *et al.*, 2021). Below, we zoom in on the Anatolian segment and attempt to identify where the various slabs predicted by plate reconstructions may currently reside.

2.2 Tethyan subduction history in the Anatolian segment

The Anatolian segment of the Alpine-Himalayan mountain belt (Figure 1) is mostly concentrated in present day Turkey. A former transform boundary with the Balkan segment has been reconstructed around the border with the Aegean region, to the west of which a double band of Jurassic ophiolites (the West and East Vardar Ophiolites, Figure 2) reveal a markedly different intra-Neotethyan subduction history than to the east (Schmid *et al.*, 2020, Maffione and van Hinsbergen, 2018). To the east, the Anatolian segment is delineated from the Iranian segment by a NNE-SSW trending fault (Figure 2) that almost coincides with the Turkey-Iran border where it coincides with the Arax Fault and its southern continuation (Allen *et al.*, 2011, Karakhanian *et al.*,

2004, van der Boon *et al.*, 2018). The Anatolian orogen is presently separated from Eurasia in the north by the Black Sea that forms a Cretaceous back-arc basin system (Okay *et al.*, 1994, Munteanu *et al.*, 2011). To the southwest of Cyprus, it is still separated by the Herodotus Basin ocean floor of the African plate (Granot, 2016), and on Cyprus and east-wards, Anatolia has undergone collision with African and Arabian plates since the late Miocene (Okay *et al.*, 2010, McPhee and van Hinsbergen, 2019, Cavazza *et al.*, 2018, Hüsing *et al.*, 2009) (Figure 2).
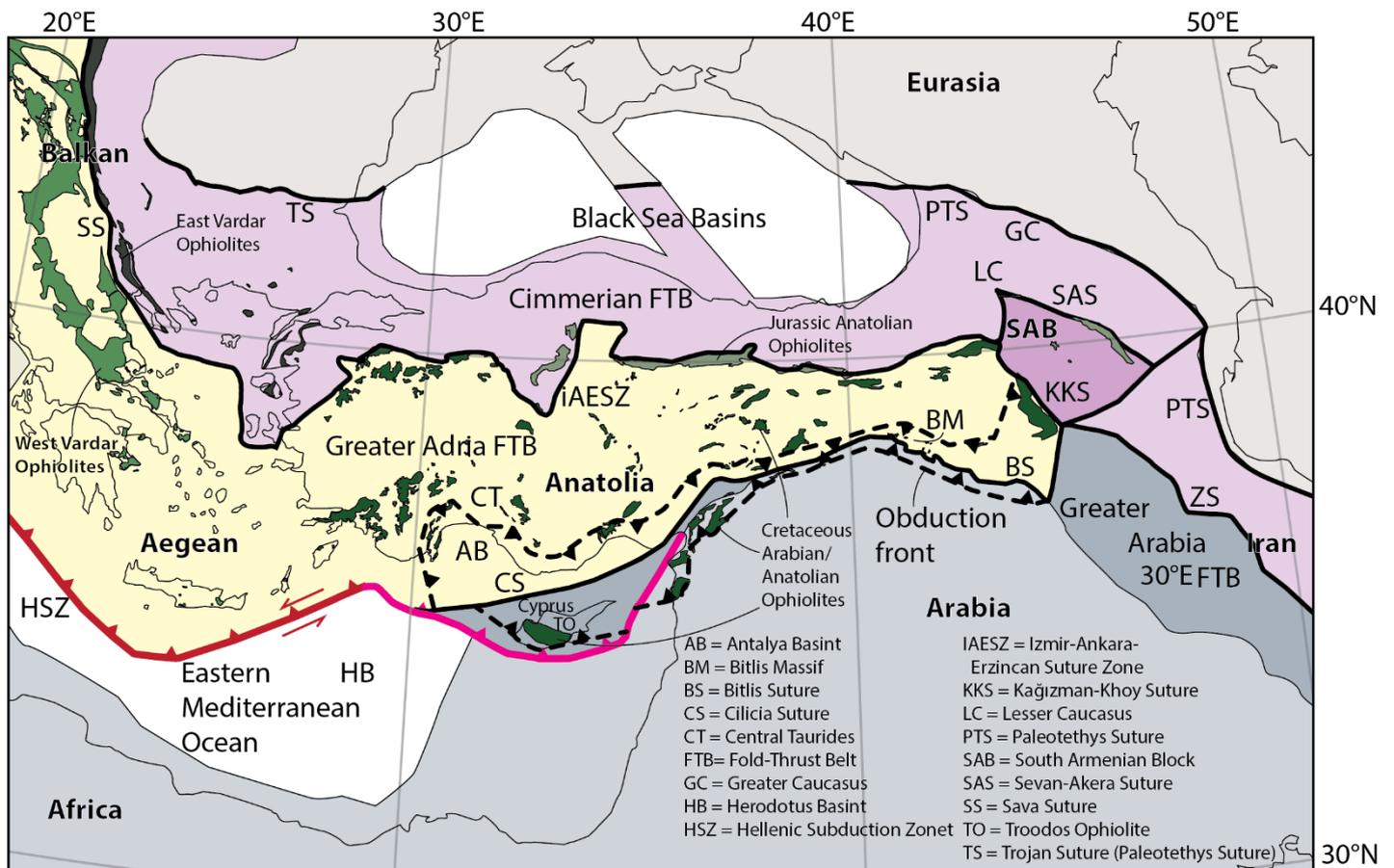

Figure 2. Simplified tectonic map of the eastern Mediterranean region, outlining the major continents, sutures, ophiolite belts, and fold-and-thrust belts derived from the Arabian continental margin and Greater Adria microcontinental realm. Modified after van Hinsbergen et al. (2020).

The Paleotethys suture has mostly been overprinted by the Cretaceous-Paleocene Black Sea rifting and opening, but Paleozoic oceanic relics accreted in Triassic to early Jurassic time below continental rocks of the Pontides are thought to be Paleotethys remnants (e.g., Şengör and Yilmaz, 1981, Dokuz *et al.*, 2017, Ustaömer and Robertson, 1999, 2010). Subduction of the Paleotethys was likely southward below the Pontides (i.e., the Cimmerian fold-thrust belt in Figure 3) (Şengör and Yilmaz, 1981), but also northward subduction likely occurred, as suggested by accretionary prism on Crimea and arc rocks in southern Russia (Okay and Nikishin, 2015) (Figure 3). Paleotethys closure is thought to have occurred in the mid-Jurassic, followed by switch to northward subduction along the southern Pontide margin and the onset of long-lived

northward subduction that lasted until the Paleogene (Robertson *et al.*, 2012, Dokuz *et al.*, 2017, Okay *et al.*, 2013) (Figure 3). The accretionary record of this subduction zone are found in the Izmir-Ankara-Erzincan suture zone (Şengör and Yilmaz, 1981) (Figure 2), in which the oldest radiolarian cherts date back to the Triassic, which is generally interpreted as the time of onset of opening of the Neotethys ocean (Tekin and Göncüoglu, 2007, Tekin *et al.*, 2002). Subduction below the Pontides terminated in latest Cretaceous time in the west (Mueller *et al.*, 2019, 2022), Paleocene time in the center (Kaymakci *et al.*, 2009), and possibly as late as early Miocene in the east, where the Neotethys was wider (Gürer and van Hinsbergen, 2019) (Figure 3).

South of the Izmir-Ankara-Erzincan Suture Zone accreted fragments of the Greater Adria continental realm, are known as the Anatolide-Tauride units in Anatolia. These continental units are overlain by upper Cretaceous supra-subduction zone ophiolites that form widespread klippen (Figure 2). These formed in the forearc of an intra-oceanic subduction zone that initiated within the Neotethys ocean in the late Cretaceous (Dilek *et al.*, 1999, Robertson, 2002, 2004, Çelik *et al.*, 2006). This subduction zone spans from triple junction around the Greece-Turkey border in the west, via a stepped fashion of segments that followed the Greater Adriatic and Arabian passive margin and perpendicular segments along former transform faults/fracture zones, towards the west Indian Ocean (Gürer *et al.*, 2016, Maffione *et al.*, 2017, van Hinsbergen *et al.*, 2021) (Figure 3). Although the segments of this intra-oceanic subduction system together formed a coherent plate boundary, its geometry evolved through time. Initially, the subduction zone had a strongly stepped, saw-tooth configuration (Maffione *et al.*, 2017). Beginning in the Late Cretaceous, trench roll-back of several segments – accompanied by extension in the overriding plate (van Hinsbergen *et al.*, 2016, Gürer *et al.*, 2018, Maffione *et al.*, 2017) – progressively smoothed this geometry. One such segment developed along the transform fault system that separated the Anatolian and Iranian segments, rolled back westwards and invaded the eastern Mediterranean ocean (Maffione *et al.*, 2017, Moix *et al.*, 2008) (Figure 3 B, C). This rollback culminated in the emplacement of ophiolites over the northwest Arabian margin of Turkey and Syria, over the extended north African margin emplacing the Troodos Ophiolite of Cyprus, as well as over the southern Greater Adrian margin (Maffione *et al.*, 2017, Inwood *et al.*, 2009, Morris and Anderson, 2002) (Figure 2, 3). Ophiolite emplacement, and likely associated slab detachment, occurred in the latest Cretaceous (Robertson and Woodcock, 1984, Al-Riyami *et al.*, 2002, McPhee and van Hinsbergen, 2019).

The Greater Adria microcontinental realm, now found in western and central Anatolia, entered the intra-Neotethyan subduction zone around 90 Ma, i.e. within a few million years of subduction initiation, and around 80-70 Ma in eastern Anatolia, as shown by the oldest metamorphosed accreted continental margin rocks (van Hinsbergen *et al.*, 2016, Topuz *et al.*, 2017, Pourteau *et al.*, 2013, 2019, Whitney and Hamilton, 2004, Whitney *et al.*, 2003). Subsequently, the entire microcontinent subducted, leaving only its upper crust, or in part perhaps its entire crust, accreted to the orogen (van Hinsbergen *et al.*, 2025). Continued microcontinental subduction is reflected by stepwise accretion of continent-derived thrust slices in the
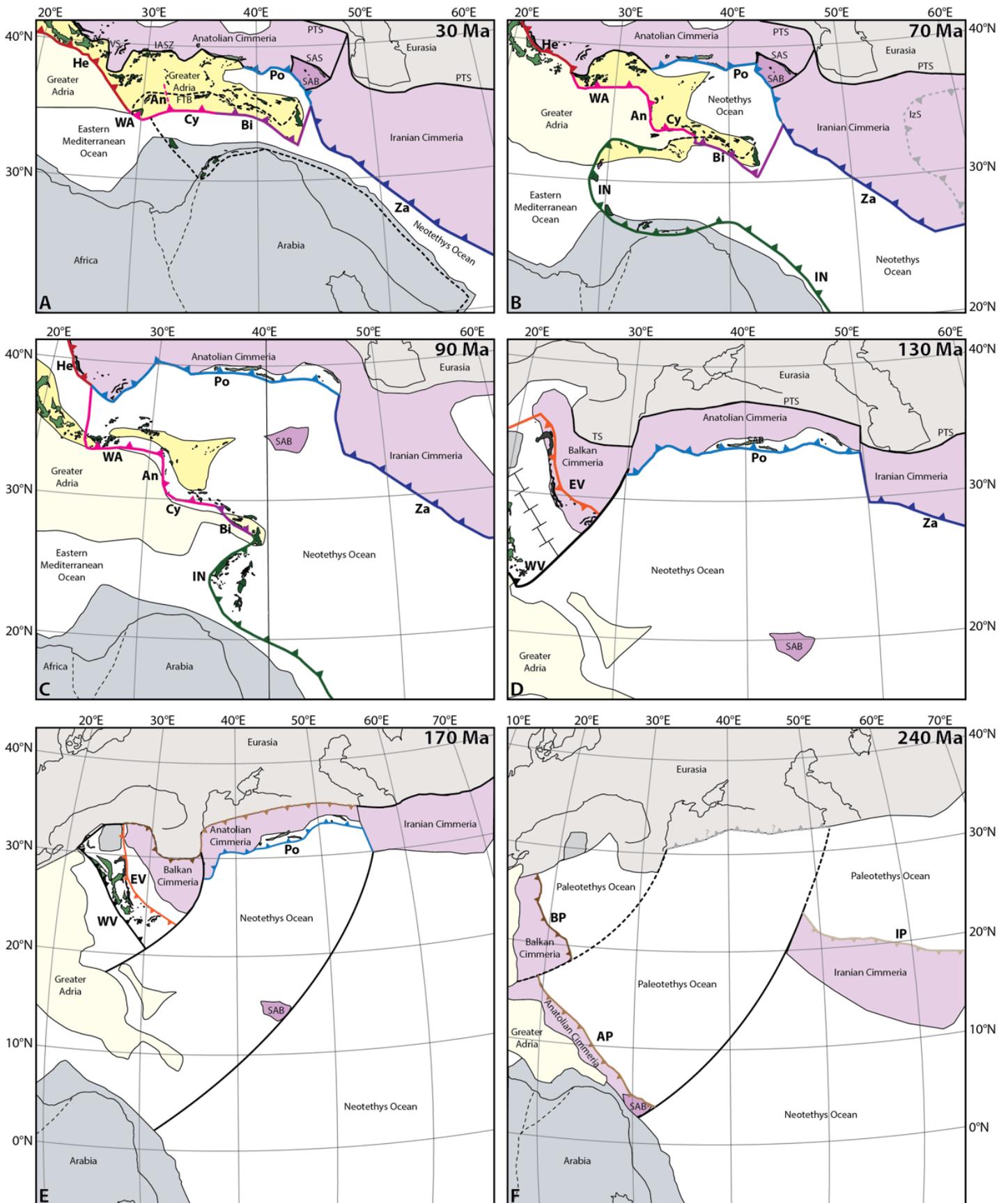
Figure 3. Tectonic reconstruction and plate boundary evolution of the eastern Mediterranean region and the Middle East used in this study as basis for tomographic interpretation. Based on van Hinsbergen et al. (2020), with additions for Iran (beyond the scope of the interpretation in this paper) from Lom and van Hinsbergen (2026), placed in the minimum-continent-motion mantle reference frame of Wagenaar et al.

Taurides orogen that occurred from the late Cretaceous until the late Eocene (McPhee *et al.*, 2018, Özgül, 1984, Andrew and Robertson, 2002). Subsequently, the eastern Mediterranean oceanic lithosphere started subducting. An exception occurred in the Central Taurides that formed in response to the westward retreat of a N-S striking subduction segment (Koç *et al.*, 2016, McPhee *et al.*, 2018). There is still a Benioff zone below the Central Taurides and Antalya Basin (Kalyoncuoğlu *et al.*, 2011), and a gradually westward moving uplift and subsidence pattern throughout the Neogene may indicate that a portion of the pre-Eocene slab is still attached and is slowly delaminating the foreland (Koç *et al.*, 2016, McPhee and van Hinsbergen, 2019).

Eastern Mediterranean oceanic crust that subducted to the south of Anatolia after the late Eocene consistent mostly of late Cretaceous back-arc basin rocks that formed in the upper plate of earlier westward invading subduction system that emplaced ophiolites over north Africa and NW Arabia. Eastern Mediterranean oceanic lithosphere subduction occurred until the arrival of the Arabian continental margin in the trench, in the Early Miocene in eastern Anatolia south of the Bitlis Massif (Cavazza *et al.*, 2018, Okay *et al.*, 2010), in the middle Miocene at the NW Arabian margin (Hüsing *et al.*, 2009), and in the late Miocene at the longitude of Cyprus (McPhee and van Hinsbergen, 2019). This accreted some of the Arabian and north African margin rocks including previously obducted ophiolites to the Anatolian overriding plate, such as in Cyprus (McPhee and van Hinsbergen, 2019). Subduction along the Arabian margin ceased, likely in the Miocene (Faccenna *et al.*, 2006, Şengör *et al.*, 2003). Ongoing convergence from Cyprus to the west is still accommodated by African plate subduction, but to the east, post-mid-Miocene convergence was accommodated in the upper plate by shortening (van Hinsbergen *et al.*, 2024) and extrusion (Şengör *et al.*, 2003, Whitney *et al.*, 2023), as well as subduction of a narrow back-arc basin north of the Pontides and its eastern continuation, the Lesser Caucasus, forming the Greater Caucasus in the process (Cowgill *et al.*, 2016).

The subduction history to the west and east of the Anatolian segment was markedly different. To the west, in the Balkan Segment, Paleotethys closure was probably simultaneous with the Anatolian segment, also ending in the middle Jurassic (van Hinsbergen *et al.*, 2020), but associated convergence was less, and the difference was accommodated by the transform fault separating the segments (Maffione and van Hinsbergen, 2018). A particular difference is that in Jurassic time, two, oppositely dipping intra-oceanic

subduction zones formed close to the mid-Neotethyan ridge bounded in the east by the transform with the Anatolian segment (Maffione and van Hinsbergen, 2018). This led to ophiolite emplacement onto both Greater Adria (West Vardar Ophiolites) and Eurasia (East Vardar Ophiolites) in late Jurassic to early Cretaceous time (Schmid et al., 2020, Tremblay et al., 2015), after which the associated slabs likely broke off. The Cretaceous intra-oceanic subduction zone that emplaced ophiolites over Greater Adria in the Anatolian segment ended against the Balkan-Anatolian transform fault and never continued much farther west (van Hinsbergen et al., 2020, Handy et al., 2010). Instead, since the middle Cretaceous, Africa-Europe convergence was accommodated by a single, north-dipping subduction zone that formed the Sava Suture in the late Cretaceous and accommodated continental subduction of Greater Adria after that until the Miocene, after which eastern Mediterranean oceanic lithosphere subducted (Menichelli et al., 2025, Schmid et al., 2020, Ustaszewski et al., 2010). This is the Hellenic subduction zone that is still active today (van Hinsbergen et al., 2005, Jolivet and Brun, 2010) (Figure 2). To the east, in Iran, Paleotethys subduction ended already in late Triassic time with the collision of the Cimmerian continent with Eurasia (Şengör, 1990, Muttoni et al., 2009, Wilmsen et al., 2009, Zanchi et al., 2009). Subsequently, Neotethys subduction started in late Jurassic time along the southern margin of the Cimmerian continent and continued until the arrival of the Arabian margin in the trench in the Oligocene (Agard et al., 2011, Mohajjel and Fergusson, 2014). The Cretaceous intra-Neotethyan subduction zone also existed in the Iranian segment and ceased in the late Cretaceous with emplacement of ophiolites along the Arabian margin (Al-Riyami et al., 2002, Moghadam and Stern, 2011). Finally, the Cimmerian continent of Iran became extended in late Jurassic and Cretaceous time, opening a partly oceanic back-arc basin, which subducted when it became invaded by continental blocks that were extruded from the Tibetan orogen in the late Cretaceous to Eocene, forming suture zones within the Cimmerian fold-and-thrust belt of Iran (Bagheri and Gol, 2020, Lom and van Hinsbergen, 2026, Berberian and Berberian, 1981).

3. Mantle structure beneath the Eastern Mediterranean and Middle Eastern region

The mantle structure of the Eastern Mediterranean and Middle Eastern region, mostly focused on the upper mantle, has previously been imaged at a variety of scales with different tomographic methods (Auer et al., 2014, Piromallo and Morelli, 2003, Li et al., 2008, Zhu et al., 2012, van der Meer et al., 2010, van Hinsbergen et al., 2010, Portner et al., 2018, Mumladze et al., 2015, Biryol et al., 2011, Govers and Fichtner, 2016, Abdelwahed, 2025, Toyokuni and Zhao, 2025, Wortel and Spakman, 2000, Kounoudis et al., 2020; see review by Faccenna et al., 2014). Geological interpretation of lower mantle structure has so far only been carried out

in detail for western Turkey (van Hinsbergen *et al.*, 2010), or as part of Tethys-wide interpretation of the mantle (van der Meer *et al.*, 2010, Wang *et al.*, 2023).

As basis for our interpretation of mantle structure, we use the global *P* wave tomography model (UU-P07 (Amaru, 2007, Hall and Spakman, 2015)). This tomographic model was previously shown to resolve slab-like features in the upper and lower mantle below the eastern Mediterranean and Middle Eastern region (van der Meer *et al.*, 2018, see https://www.atlas-of-the-underwold.org/download for sensitivity tests). Moreover, this model has been used for the global slab-geology correlations that underpin the estimation of global slab kinematics in the mantle (van der Meer *et al.*, 2018).

We placed our reconstruction in a mantle reference frame (Figure 3) based on the assumption of minimum-continent-motion, a model that predicts hotspot motions well (Wagenaar *et al.*, 2025). Significant mispredictions of slab locations by this model may then be interpreted as evidence for significant post-breakoff horizontal slab motion. The paleo-subduction zones of the Anatolian Tethys Ocean segment advanced and rolled back through areas currently occupied by the Aegean, Anatolia, the Ionian-Herodotus Basin, NW Arabia, and North Africa. If slabs following their detachment did not substantially move laterally, the record of Anatolian Tethyan subduction is expected to be found in N(E)-S(W) transects in the mantle below, from the Black Sea to north Africa. Slabs that formed in the Iranian segment are then expected to the east as previously described (van der Meer *et al.*, 2010, 2018, Agard *et al.*, 2011), and of the Balkan segment to the west (Maffione and van Hinsbergen, 2018, Handy *et al.*, 2010). From those adjacent segments, we only indicate where previously described prominent anomalies reside as reference for our further interpretation. We study anomalies in a series of N-S cross-sections, from west to east (Figure 4), in addition to horizontal cross sections at 200 km depth intervals. These N-S sections are sub-parallel to the overall long-lived convergence direction in the eastern Mediterranean region but may cut obliquely through slabs that formed at westward retreating, east-dipping trenches in the reconstruction. We catalogue upper and lower mantle anomalies and indicate whether these were identified before. We use the nomenclature convention of van der Meer *et al.* (2018), naming anomalies using their modern geographic location, rather than the lithosphere that we interpret it may represent. In a following section, we interpret how these anomalies may be linked to the reconstructed subduction history.
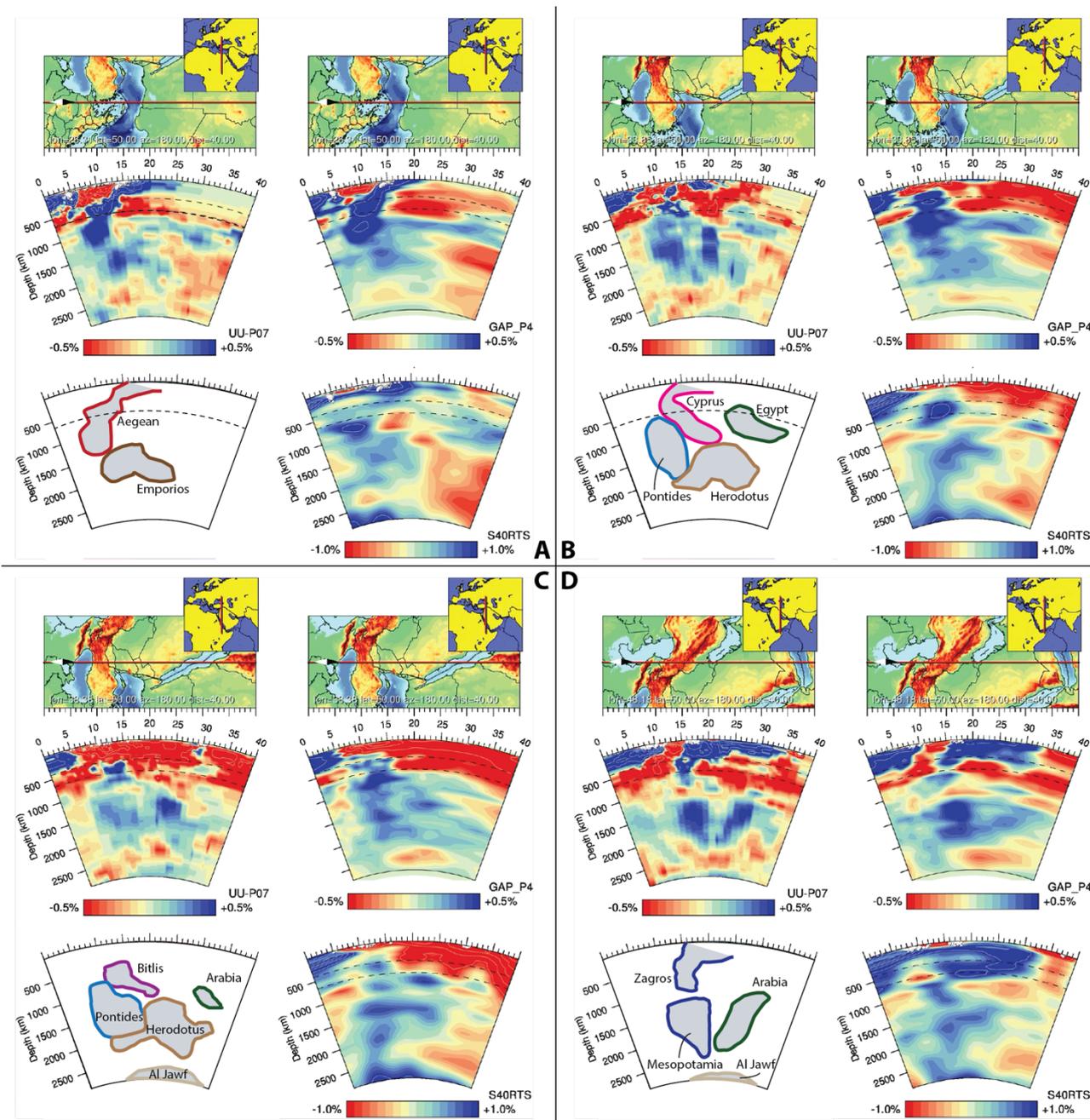
Figure 4. Tomographic cross sections of the upper and lower mantle below the Eastern Mediterranean region, from seismic tomographic models UU-P07 (Amaru, 2007, Hall and Spakman, 2015), GAP_P4 (Obayashi et al., 2013) and S40RTS (lower mantle) (Ritsema et al., 2011). Interpretated anomalies are based on the UU-P07 images. A) Aegean section; B) Cyprus section; C) Bitlis section; D) Western Iran section.

The *Aegean anomaly* (Figure 4a) is the most prominent anomaly of the southeastern Balkan section. Its upper mantle part was first imaged by Spakman (1986) and Spakman *et al.* (1988) and was later shown to penetrate the lower mantle, reaching a depth of ~1500 km below northern Greece (Bijwaard *et al.*, 1998, van Hinsbergen *et al.*, 2005, Spakman *et al.*, 1993). It is still connected to the subducting African plate and is thus commonly interpreted as subducted African plate lithosphere (Biryol *et al.*, 2011, Chang *et al.*, 2010, van Hinsbergen *et al.*, 2005, 2010, Spakman *et al.*, 1988, Piromallo and Morelli, 1997, Hafkenscheid *et al.*, 2006, Faccenna *et*

al., 2003, De Boorder *et al.*, 1998). Below 660 km, the slab is about twice as thick as in the upper mantle, likely due to slab shortening upon deceleration when entering the lower mantle (van Hinsbergen et al., 2005). Towards the east, the Aegean slab continues below western Turkey, where it has broken off from the African plate as shown by an upper mantle slab gap (Figure 4b) (Biryol *et al.*, 2011, van Hinsbergen *et al.*, 2010, Portner *et al.*, 2018).

Below and south of the southern tip of the Aegean anomaly lies the *Emporios anomaly* (Figure 4a). This anomaly is in the lower mantle, between ~1500-2000 km and seems to dip to the south (van der Meer *et al.*, 2018). This anomaly was interpreted as contiguous with the Aegean anomaly, perhaps linked to deep folding of the slab (Faccenna *et al.*, 2003), whereas van Hinsbergen *et al.* (2005) interpreted it as a separate anomaly.

The *Cyprus anomaly* (Figure 4b) was identified by Faccenna *et al.* (2006), Biryol *et al.* (2011), Portner *et al.* (2018), van der Meer *et al.* (2018), and McPhee *et al.* (2022). It is still connected to African plate lithosphere that is subducting at the trench south of Cyprus and is thus commonly inferred to represent subducted African plate lithosphere. This lithosphere may be in the process of breaking off north of Cyprus (Portner *et al.*, 2018). The Cyprus anomaly has a northward dip in the upper mantle. To the east, the upper mantle portion of the Cyprus anomaly abruptly ends around ~35.5° longitude which coincides with the location of the boundary between the central and eastern Taurides. The anomaly appears to continue into the lower mantle down to ~1000 km (van der Meer et al. 2018), where and seems to be overturned in the transition zone, below which it dips southward in the lower mantle (Figure 4b).

To the south of the Cyprus anomaly, in the upper part of the lower mantle between ~900 and 1300 km, lies the *Egypt anomaly* (Figure 4b, c). It was first identified by Hafkenscheid *et al.* (2006). It was included under that name in the compilation of van der Meer *et al.* (2010) but was later considered the westernmost part of a WNW-ESE trending set of anomalies that extends across below southeast Arabia - the Arabian anomalies of van der Meer *et al.* (2018). This Egypt anomaly is sub-horizontal below a wide region spanning present day Egypt and northern Sudan between ~22-35°, to possibly as far west as the Aegean Anomaly (Figure 4b, c).

To the east of the Cyprus anomaly, below northernmost Arabia just south of the Bitlis suture zone, lies the *Bitlis anomaly* (Figure 4 c). This anomaly, also identified by e.g., Hafkenscheid *et al.* (2006), Faccenna *et al.* (2006), Lei and Zhao (2007), Zor (2008), and van der Meer *et al.* (2018), is found at a depth of up to ~900 km up to the mantle transition zone, ~500 km depth and is no longer connected to continental crustal lithosphere.

All N-S sections across Anatolia reveal a thick, sub-vertical high-velocity body below central and northern Turkey and the southern Black Sea, from the top of the lower mantle around 600-700 km down to ~2000 below western Turkey, increasing to 2200 km and thickening towards the east (Figure 4b, c): this is the *Pontides anomaly*. It is considerably thicker and reaches greater depth than the upper mantle portions of the

Cyprus and Aegean slabs. It is similar in N-S lateral width as the lower mantle portion of the Aegean anomaly, suggesting it may represent equally thickened lithosphere.

A distinct anomaly is in the lower mantle to the south of the Pontides anomaly and beneath the Egypt anomaly, between ~1500 or perhaps even some hundred kilometers shallower, and 2200 km depth and between ~15 and 30°N (Figure 4b, c). This feature is identified as the *Herodotus anomaly* based on its present-day location below the Herodotus Basin (Figure 2, 4b, c). The anomaly has a sub-horizontal base. The tomographic images show significant thickening of this body. Westwards, the anomaly may be connected to the Emporios anomaly.

To the east, below Iran, van der Meer *et al.* (2010, 2018) identified the prominent, thick *Mesopotamia anomaly* (anomaly II in Van der Voo *et al.* (1999b)). This anomaly is located between ~1100 and 2200 km depth (Figure 4d). Above it, the *Zagros anomaly* is a northward dipping anomaly in the upper mantle (Hafkenscheid *et al.*, 2006, Zor, 2008, Chang *et al.*, 2010, Agard *et al.*, 2011, Koulakov, 2011) that reaches lower mantle depths of ~1000 km (Figure 4d). The Zagros slab is disconnected from the deeper Mesopotamia slab, and it also displays a gap at the top, suggesting it has lost its connection to the lithospheric plates at surface. To the south (Hafkenscheid *et al.*, 2006) identified the *Arabia anomalies* (anomaly I in Van der Voo *et al.* (1999b)) in the upper part of the lower mantle. They continue to the SE from the Egypt anomaly, in the mid-mantle below ~1100 km.

On the core-mantle boundary below Arabia lies the *Al Jawf anomaly* (van der Meer *et al.*, 2018) reaching up to ~2500 km depth. This anomaly disappears westward below Anatolia and is detectable until the Bitlis segment (Figure 4c, d) in the UUP07 model.

Finally, there are two smaller anomalies in the upper mantle below the eastern Mediterranean region that we do not specifically show here, and that have been interpreted to play a role in the Cenozoic history of the region. First, to the northwest of the Cyprus anomaly, below the Central Taurides and currently isolated from active plate boundaries, is the *Antalya anomaly*. This anomaly was identified by De Boorder *et al.* (1998), Biryol *et al.* (2011), van der Meer *et al.* (2018), and McPhee *et al.* (2022) and is a NNW-SSE striking, eastward dipping high-velocity anomaly, associated with a diffuse Benioff zone (Kalyoncuoğlu *et al.*, 2011), below the western Central Taurides. At depths exceeding ~300-400 km, the Antalya anomaly becomes tomographically indistinguishable from the Cyprus anomaly. Finally, to the northeast of the Pontides anomaly, the north-dipping *East Caucasus anomaly* is connected to the lithosphere and reaches a depth of ~300 km (Maggi and Priestley, 2005, Mumladze *et al.*, 2015). Below the west-Caucasus, there is no such anomaly connected to the surface, but instead, the *West Caucasus anomaly* is imaged in the mantle transition zone, decoupled from the lithosphere (Hafkenscheid *et al.*, 2006, Zor, 2008, Koulakov *et al.*, 2012, van der Meer *et al.*, 2018). We refer to reader to the cited sources for detailed images of these anomalies, resulting from late Cenozoic-present subduction, which play only a subordinate role in our interpretation here of the older Tethyan ocean.

4. Correlating reconstruction and tomography

4.1 Concepts and assumptions

To interpret which anomalies imaged by tomography in the mantle below the eastern Mediterranean region and Middle East may correspond to subducted lithosphere reconstructed from surface geology, we first introduce a few previously developed concepts and assumptions that consider slab shape and depth (Figure 5). First, we interpret shallower anomalies as younger, and deeper anomalies as older slabs. Second, we assume that after slab detachment, slabs did not change lateral position relative to each other. In other words, anomalies that are currently located north and south from each other in the mantle are interpreted as slabs that subducted north and south from each other, respectively. Third, as a guide, we use previously reconstructed global subduction rates that suggested that all upper mantle slabs represent Cenozoic subduction and older slabs have sunken into the lower mantle, and that it takes ~250 million years for slabs to sink down to the core-mantle boundary (van der Meer *et al.*, 2010, 2018, Butterworth *et al.*, 2014) to hypothesize that the anomalies we identified above represent all subducted Paleotethyan and Neotethyan lithosphere of the Anatolian segment and in the adjacent segments. Fourth, slabs that subduct at upper mantle rates that exceed lower mantle sinking rates thicken by buckling at in the mantle transition zone and in the upper part of the lower mantle (Sigloch and Mihalynuk, 2013, Wu *et al.*, 2016, Pokorný *et al.*, 2021, van der Wiel *et al.*, 2024a, Chen *et al.*, 2019, Fuston and Wu, 2021, Pownall *et al.*, 2017, van der Meer *et al.*, 2018). Lower mantle slabs therefore are typically much thicker than upper mantle slabs and may contain considerably more subducted lithosphere than suggested by their vertical length alone.

In addition, previous analyses have shown that modern slab geometries may reveal past trench motions during subduction (Sigloch and Mihalynuk, 2013, Qayyum *et al.*, 2022, Parsons *et al.*, 2020, Wu *et al.*, 2016, Schellart, 2005) (Fig. 5). Slabs subducted at mantle-stationary trenches typically appear near vertical, whereas slabs subducted at retreating trenches during the Cenozoic tend to currently still drape the 660 km discontinuity (Wortel and Spakman, 2000, Piromallo and Morelli, 2003, Čížková and Bina, 2015, Schellart, 2005). These sub-horizontal slab geometries may persist as older slabs as they continue to sink further into the lower mantle (Sigloch and Mihalynuk, 2013, Boschman *et al.*, 2018, Parsons *et al.*, 2020, Qayyum *et al.*, 2022). Moreover, slabs that subduct at advancing trenches may become overturned (Sharples *et al.*, 2014) and this shape may be preserved after detachment (e.g., the Himalaya slab (Replumaz *et al.*, 2010b, van Hinsbergen *et al.*, 2019, Qayyum *et al.*, 2022)). Finally, there may be subtle differences in sinking rate between slabs that sink at mantle stationary versus moving trenches. This is exemplified by the mantle-stationary Mariana slab, that subducted to ~1200 km since the inception of subduction around 60-50 Ma, and the adjacent Izu-Bonin slab that subducted at the same trench but retreated and still lies sub-horizontally above the 660 km discontinuity (Miller *et al.*, 2005, Zhang *et al.*, 2019). The global analysis of slabs of van der Meer *et al.* (2018); their Figure 100) showed that the lower mantle sinking rate of detached

slabs is uniform, regardless of their shape. The upper mantle history of a subducting slab determines whether the slab entry (steep vs. shallow angle) in the lower mantle is delayed (sub-horizontal slabs) with respect to slabs subducting at a stationary trench. This causes a lateral spread in the age-depth inference of sinking slabs in the lower mantle and makes that sub-horizontal slabs on average sank slower.

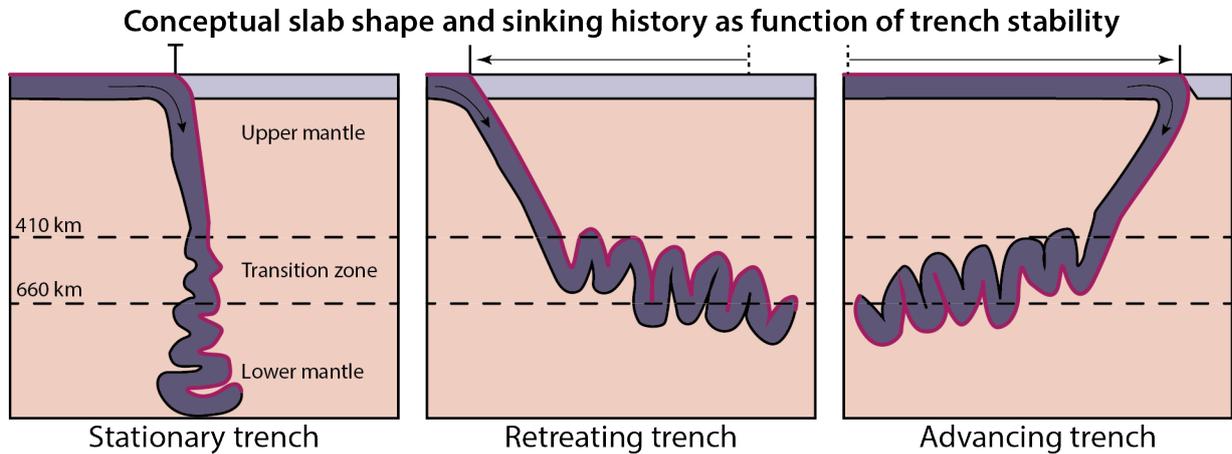**Conceptual slab shape and sinking history as function of trench stability**

Figure 5. Conceptual relationship between slab shape and sinking behavior of mantle stationary versus mobile trenches. Modified after Parsons et al. (2020) and Qayyum et al. (2022).

4.2 Interpreting eastern Mediterranean and Middle Eastern tomography

As a first guide in our correlation between tectonic reconstructions and mantle tomography of the eastern Mediterranean region and the Middle East, the actively subducting Aegean slab (Figure 4a) provides a tie point in the west, and the Zagros and Mesopotamia slabs provide a tie point in the east (Figure 4d). The architecture and reconstruction of the Aegean orogen show that the Aegean slab has been subducting for the last ~100 Ma, and with a slab thickening factor of ~1.5-2 reasonably accounts for the volume of lithosphere - both oceanic and microcontinental - that was consumed since this time (van Hinsbergen *et al.*, 2005, 2020, vJolivet and Brun, 2010). Subduction zone reconstructions in absolute plate motion context suggest that the Aegean trench has been mostly mantle-stationary throughout this history, providing a tie to the mantle frame, and only in the Neogene the trench moved significantly, due to slab roll back of a few hundred kilometers in the upper mantle. This is reflected by a sub-horizontal portion of the slab in the mantle transition zone (van Hinsbergen *et al.*, 2005, 2020, van Hinsbergen and Schmid, 2012).

The Emporios slab (Figure 4a) that is located below the Aegean slab was first interpreted as an overturned, deeply subducted portion of the Aegean slab (Faccenna *et al.*, 2003). However, taking slab thickening into account, this would require much more subduction than the ~2000 km of convergence accommodated by the Aegean subduction zone, and it would suggest that the pre-100 Ma subduction that occurred in the Balkan segment (Figure 3) would be unaccounted for in seismic tomography. Van Hinsbergen *et al.* (2005) interpreted the Emporios slab as oceanic lithosphere that was subducted below the West Vardar

Ophiolites in the Jurassic. However, reconstructions show that this slab likely broke off at a location below modern northern Africa, where it may correspond to the Algeria slab (van der Meer *et al.*, 2010), not shown in our cross sections of Figure 4. Van der Meer *et al.* (2018) therefore suggested that the Emporios slab corresponds to the lithosphere subducted below the East Vardar ophiolites. However, it is questionable whether sufficient lithosphere subducted in this subduction zone (see also Schmid *et al.*, 2020), and this lithosphere may instead be in the deeper part of the Aegean anomaly, undiscernible from the Hellenic slab. We follow the latest interpretation, of Maffione and van Hinsbergen (2018), that the Emporios slab represents Paleotethyan lithosphere that was consumed during the Triassic to middle Jurassic opening of the Neotethys Ocean in the Balkan segment.

To the east, the Zagros slab (Figure 4d) is widely interpreted to reflect Arabian plate lithosphere that subducted below the Iranian Cimmerian terranes (e.g., Agard *et al.*, 2011, Rahmani *et al.*, 2019, Veisi *et al.*, 2021). Below much of the Zagros belt, this slab is detached from the Arabian plate (but not below the Makran (Qayyum *et al.*, 2022)), and slab detachment is thought to have occurred ~10 Myr ago based on high-silica adakites above the imaged slab gap (Omrani *et al.*, 2008, Chiu *et al.*, 2013, Agard *et al.*, 2011). The East Caucasus anomaly (not indicated in Figure 4, see van der Meer *et al.* (2018)) is interpreted as the back-arc basin lithosphere that reconstructions show subducted below the Greater Caucasus since the late Eocene (Cowgill *et al.*, 2016), whereby the West Caucasus anomaly is thought to reflect a portion of that slab that detached, likely 5 Ma ago (Forte *et al.*, 2014, Avdeev and Niemi, 2011).

Geological reconstructions suggest that there has been continuous subduction along the Zagros subduction zone since the Late Jurassic, consuming far more lithosphere than the ~1000 km accounted for by the Zagros slab. The Mesopotamia slab (Figure 4d) is thus interpreted to also reflect subduction of Neotethys lithosphere (van der Meer *et al.*, 2010, 2018). The cause of the decoupling of the Zagros and Mesopotamia slab is not known. It has been suggested that it may have coincided with latest Cretaceous to Paleogene rapid exhumation of HP-LT metamorphic rocks in the Zagros suture zone (Agard *et al.*, 2011). Alternatively, it may coincide with the arrival of the Neotethyan ridge in the trench, in which case it likely occurred in the early Cretaceous (Stampfli and Borel, 2002). Either way, kinematic reconstruction of the tectonic evolution of the Iranian segment (Lom and van Hinsbergen, 2026) placed in the minimum-continent-motion mantle reference frame (Wagenaar *et al.*, 2025) suggest that the Mesopotamia and Zagros slabs subducted at a mostly mantle-stationary trench. To the south, the Arabia anomalies likely candidates to be the slab remnants of the intra-Neotethyan subduction zone that formed in the late Cretaceous and culminated with ophiolite emplacement onto the Arabian margin in latest Cretaceous time (Agard *et al.*, 2011, van der Meer *et al.*, 2018). We note, that this requires that the Arabia slabs sank quicker than the Mesopotamia slab - in fact, these are among the few fastest sinking slabs in the global documentation of van der Meer *et al.* (2018), at rates of ~2 cm/yr, but in absence of any other known Mesozoic subduction to the south of the Zagros subduction zone, the late Cretaceous Intra-Neotethyan subduction zone is the only

candidate to explain this slab. Van der Meer et al. (2018) speculated that elevated mantle temperatures close to the edge of the African LLSVP may locally cause lowered mantle viscosity and enhanced slab sinking. The Egypt slab, which has the same age and subducted as a segment of the same overall subduction zone, is much shallower in the mantle, which we interpret as the result of its roll-back into the eastern Mediterranean Ocean, decreasing its overall sinking rate (Fig. 5).

Finally, the Al Jawf slab, draping the core-mantle boundary to the south of the Mesopotamia slab, was previously interpreted to account for the Paleotethys ocean of the Anatolian segment (van der Meer et al., 2018). However, both its greater depth, and the longitudinal separation from the Emporios slab makes it more likely that the Al Jawf slab (Figure 4d) represents lithosphere of the Iranian Paleotethys ocean, that closed between late Permian and late Triassic time.

These correlations of the Aegean and Emporios, and Zagros-Mesopotamia and Al Jawf slabs thus suggest that the Cyprus, Egypt, Antalya, Pontides, Arabia, and Herodotus anomalies (Figure 4b, c) account for the Tethyan lithosphere that subducted in the Anatolian segment. If the Aegean and Mesopotamia-Zagros slabs subducted at more or less mantle-stationary trenches, their maximum depth and age (~1400 km in ~100 Ma for the Aegean slab, ~2200 km in ~150 Ma for the Mesopotamia slab) may be used as guide to interpret the slabs of the Anatolian segment, bearing in mind that slabs that subducted at moving trenches likely were delayed in entering the lower mantle which may amount to a delay of 60-50 Myrs compared to the slabs subducting at stationary trenches (see discussion concerning Figure 100 in van der Meer et al. (2018)).

Our plate tectonic reconstruction shows that subduction along the Pontides trench was also mostly mantle-stationary and occurred between ~180-170 and ~60 Ma (or younger, early Miocene in the east (Gürer and van Hinsbergen, 2019)). Based on global correlations (van der Meer et al., 2018) and the correlations between reconstructions and tomography in the Aegean and Iranian segments (van der Meer et al., 2010, Maffione and van Hinsbergen, 2018), the associated slab (Figure 4b, c) is thus expected to be vertical, thickened, and located between the deep mantle and the mantle transition zone. This prediction fits well with the location and depth of the Pontides slab between ~2000-2200 and ~600 km (1400-1600 km vertical length). The tectonic reconstruction (Figure 3) shows that from west to east, ~1500-3000 km of lithosphere subducted northward below the Pontides (or more if spreading in the Neotethys ocean continued during subduction), requiring a thickening factor of up to 2 for the Pontides slab, which we consider reasonable considering the outlined shapes in Figure 4b and c.

Lithosphere that subducted at the trench within the Neotethys Ocean since the late Cretaceous has likely sunken into the lower mantle (van der Meer et al., 2018). Moreover, our reconstruction in an absolute plate motion frame (Wagenaar et al., 2025) suggests that the trench at which this lithosphere subducted has advanced northwards over ~1000 km since its initiation in the late Cretaceous, while consuming ~1300 km of lithosphere (cf. Figure 5). Because this trench currently coincides with the Cyprus trench (van Hinsbergen et al., 2020), we may thus expect a slab of this length, or shorter if thickened, to extend from the Cyprus

subduction zone downwards, and to be overturned because of the trench advance and the limited length of the trench. The Cyprus anomaly (Figure 4b, c) fits this prediction well. Its base around 1000 km is located ~300-400 km below the top of the Pontide slab, consistent with the reconstruction that these slabs underwent a period of simultaneous, double same-dip subduction since the late Cretaceous. Moreover, the Cyprus slab is overturned in the lower mantle (until ~1000 km depth) and has a length that corresponds well to the reconstructed amount of subducted lithosphere.

Following earlier interpretations, we infer that the Antalya anomaly (see van der Meer *et al.*, 2018, Biryol *et al.*, 2011 for images), which becomes indiscernible from the Cyprus anomaly in the mantle transition zone, represents lithosphere that subducted at a N-S trending segment of the subduction zone that formed in the Cretaceous Neotethys, and that became isolated from the African plate in the late Eocene when lithosphere of the Menderes-Bey Daglari foreland delaminated and the trench jumped to the south of Greater Adria (van Hinsbergen *et al.*, 2010, 2025). The Antalya slab has been slowly delaminating and detaching since then (McPhee *et al.*, 2019, Koç *et al.*, 2016). Similarly, to the east we follow previous interpretations that link the Bitlis anomaly below northernmost Arabia to the lithosphere that broke off northern Arabia following the arrival of the Arabian margin in the trench in the middle to late Miocene (e.g., Faccenna *et al.*, 2006, Keskin, 2003, Şengör *et al.*, 2003, Lei and Zhao, 2007).

Slab remnants that formed due to the westward roll-back of an east-dipping segment of the late Cretaceous intra-Neotethyan subduction zone into the Eastern Mediterranean Ocean that culminated in ~70-65 Ma ophiolite emplacement onto the NW Arabian, NE African, and south Greater Adrian margin are expected to be located south of the Cyprus subduction zone. Given the roll-back history, this slab is expected to be of sub-horizontal shape located in the upper part of the lower mantle. The sub-horizontal Egypt slab (Figure 4c) fits well with this prediction and is in the region where our plate reconstruction would predict the remnants.

The analysis above suggests that the Egypt, Cyprus, and Pontides slabs, together with the smaller bodies of the Bitlis and Antalya slabs, account for the Neotethyan subduction history that occurred since the middle Jurassic in the Anatolian segment. Seismic tomography reveals four major slab remnants, partly in the upper, but mostly in the lower mantle. The combined dimension of three slabs is consistent with the kinematically-restored subducted area of the Neotethys. From this it follows that the fourth and deepest lower mantle slab - Herodotus anomaly (Figure 4b, c) is unlikely to represent Neotethyan lithosphere and represents the slab remnant of Paleotethys lithosphere that subducted between ~240 and ~180 Ma. The Herodotus slab is found over a N-S distance of ~1500 km when projected to the surface, and its thickness is consistent with a factor of 2-2.5 thickening to account for the once ~3000-4000 km wide Paleotethys ocean. Moreover, our tectonic reconstruction in the mantle reference frame predicts a latitude of ~35°N for Pontides-Eurasia collision, i.e. coinciding with the northern end of the Herodotus slab. The base of the Herodotus slab is located only slightly deeper in the mantle than the Pontides anomaly suggesting it sank

slower. This is consistent with the inference that (most of) the Paleotethys ocean subducted southward, and rolled back northward (Şengör and Yilmaz, 1981), such that it likely sub-horizontally draped the mantle transition zone, had a longer upper mantle transit time, and as a result a lower net sinking rate than the Pontide slab which resulted from Neotethys subduction.

5. Discussion

Our analysis of tomographic images of the upper and lower mantle below the eastern Mediterranean region reveals that these anomalies account for the amount and location of subducted lithosphere predicted by detailed kinematic reconstructions of subduction evolution based on plate kinematics and orogenic architecture. Parts of these interpretations were provided previously, but mostly for the upper mantle (e.g., Biryol *et al.*, 2011, Confal *et al.*, 2025) or for only part of the Tethys Oceans system (Hafkenscheid *et al.*, 2006, van Hinsbergen *et al.*, 2010, Faccenna *et al.*, 2006). Upper mantle studies only account for a fraction of the subducted lithosphere, mostly linked to the Cenozoic subduction evolution, but in absence of the lower mantle portions it is not possible to identify what part of the subduction history is accounted for by upper mantle anomalies. Our analysis here suggests that almost all the lithosphere that subducted below the Pontides now resides in the lower mantle. The upper mantle portion is restricted to the Cyprus and Antalya slabs. Smaller remnants that have been proposed to reside in the upper mantle to the north of these (e.g., Confal *et al.*, 2025) may represent small lithospheric drips that delaminated in the late Cenozoic (e.g., Göğüş *et al.*, 2017).

The successful correlation between reconstructed subduction history, placed in a mantle reference frame, and seismic tomography shows that the Tethyan slabs of the Aegean and Anatolian segments sank vertically after breakoff, mostly maintaining the shape that they acquired while they were still connected to the surface plates (Figure 6). The Herodotus slab mainly subducted southwards, rolling back northwards, and likely draped the 660 km discontinuity temporarily like modern western Mediterranean slabs do (Spakman and Wortel, 2004). Following Herodotus' detachment, the Pontides slab started to subduct northwards at a mantle-stationary trench and formed a 'slab-wall' (cf. Sigloch and Mihalynuk, 2013) just to the north of the detached Paleotethys-related Herodotus slab. Around 105 Ma, when the intra-Neotethyan subduction zone initiated (Pourteau *et al.*, 2019, van Hinsbergen *et al.*, 2021), the Cyprus slab started to subduct, in tandem with the Pontides slab. Several hundreds of kilometers of the Cyprus slab must consist of continental lithosphere and formed the original lithospheric underpinnings of the nappes of the Anatolide-Tauride belt. Between ~85 and 65 Ma, and during subduction of the Cyprus slab, the Egypt slab formed to the south by westward roll-back into the eastern Mediterranean ocean, draped the transition zone, which lead to a sub-horizontal slab which was followed by latest Cretaceous slab detachment. Until the arrival of the Anatolide-Tauride orogen in the trench along the southern Pontides, the Cyprus slab converged with the

Pontides slab and overturned in the process. From 60 Ma onwards, and later in the east, the Pontides slab detached and Africa-Eurasia plate convergence was mostly accommodated by the Cyprus slab alone which is at present in the process of breaking off from the north African margin (Figure 6).
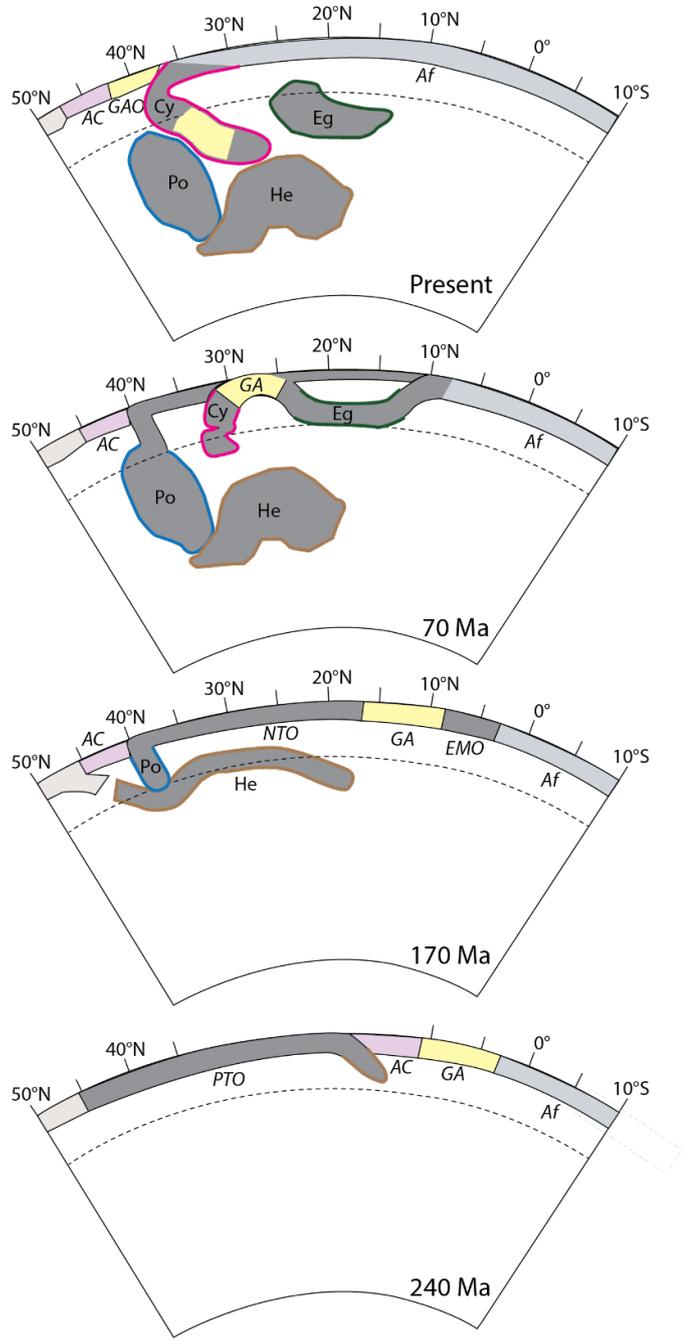
Figure 6. Interpreted evolution of eastern Mediterranean mantle structure parallel to the section shown in Figure 4B, resulting from subduction evolution of the Paleotethys and Neotethys oceans. AC = Anatolian Cimmeria; Af = Africa; Cy = Cyprus slab; Eg = Egypt slab; EMO = Eastern Mediterranean Ocean; GA = Greater Adria; GAO = Greater Adria-derived accretionary orogen; He = Herodotus slab; NTO = Neotethys Ocean; Po = Pontides slab; PTO = Paleotethys Ocean

The average slab sinking rates of Tethyan slabs reconstructed here, which penetrated the lower mantle, vary between ~1.0 and 1.5 cm/yr. These rates are on par within the range of sinking slabs globally (van der Meer *et al.*, 2010, 2018), as well as with sinking rates for the Tibetan segment (Parsons *et al.*, 2020, Qayyum *et al.*, 2022). These rates are considerably slower than plate convergence velocities reconstructed for plates approaching Eurasia during closure of the Neotethys Ocean. Africa–Eurasia convergence experienced a Late Cretaceous acceleration to ~6–8 cm/yr (e.g., Gürer *et al.*, 2022)), whereas Arabia–Eurasia convergence during the Cenozoic was typically ~2–3 cm/yr (e.g., McQuarrie *et al.*, 2003)). By contrast, the Indian plate moved substantially faster prior to collision with Eurasia, reaching velocities of up to ~15–20 cm yr^{-1} (e.g., van Hinsbergen *et al.*, 2011, Patriat and Achache, 1984, DeMets and Merkouriev, 2021). This discrepancy between plate convergence and slab sinking rates was accommodated by either bulk deformation or buckling, resulting in thickening of slabs imaged by tomography (i.e. Hafkenscheid *et al.*, 2006), also discussed in van der Meer *et al.* (2018)). The sinking of the Tethyan slabs has been suggested to stir a whole mantle convection that would contribute to driving these plate motions (Becker and Faccenna, 2011). However, the reconstructed lower mantle slab sinking rates rather suggest that ambient lower mantle sinking when induced by slab sinking must be even slower (van der Wiel *et al.*, 2024b) and therefore may only have provided a subordinate contribution to the plate motions that closed the Tethyan oceans.

Finally, the recent minimum-continent-motion mantle reference frame of Wagenaar *et al.* (2025) was developed as a reference to reconstruct mantle convective motions and may be evaluated in the light of the correlations made in this paper. This frame was developed under the explicit assumption that the ambient mantle does not undergo any motions that were not induced by plate motion, i.e. that without plate motions, it would have been stagnant. Deviations of predicted and observed locations of e.g. slabs in the mantle may thus be used to infer non-plate tectonic induced ambient mantle flow (Wagenaar *et al.*, 2025). However, the slabs of the Anatolian Tethyan segment reconstructed here are at first order straightforwardly explained by vertical, post-detachment sinking, and for now do not require significant systematic horizontal convective currents in the ambient mantle. Moreover, adjacent to our studied region towards the east, no major mantle flow is needed to connect the slabs of the Tibetan segment to their respective trenches for slabs since the Jurassic (Parsons *et al.*, 2020, Qayyum *et al.*, 2022), and the transform fault zones that bounded the Tethyan segments appear to still be reflected in mantle structure (Figure 7). This suggests that the predicted longitudinal stability of the Neotethyan realm predicted by the minimum-continent-motion reference frame explains mantle structure well, as previously inferred on a global scale (Domeier *et al.*, 2016). We see no evidence to invoke major lateral mantle 'winds', as sometimes predicted by numerical models with major mantle flow (e.g., Peng and Liu, 2022).

An exception may be the absolute position of the Tethyan subduction system for the Triassic, corresponding to the slab graveyard in the lowermost few hundred kilometers on top of the core-mantle boundary. The first-order subdivision of the main Tethyan segments (Figure 1) appears to be well-reflected by

deepest-mantle structure, but the Wagenaar et al. (2025) frame may be offset eastwards by ~10°. This may indicate that for Pangea times, the minimum-continent-motion frame, which fixes Pangea relative to the mantle because it contains almost all continental lithosphere, is oversimplified for this time interval. Alternatively, short-lived lateral mantle flow may have occurred in either the Triassic during the descent of subducted Paleotethyan slabs, or since arrival of the slabs at CMB (see e.g., Fritzell et al., 2016), have been offset by lateral mantle flow in the deepest mantle in the past ~50 Myr. However, to advance the use of seismic tomography to kinematically reconstruct motions in the mantle, a more quantitative analysis needs to be developed, with a thorough definition of slab versus ambient mantle, and quantification of uncertainties in slab location, edge, and shape.
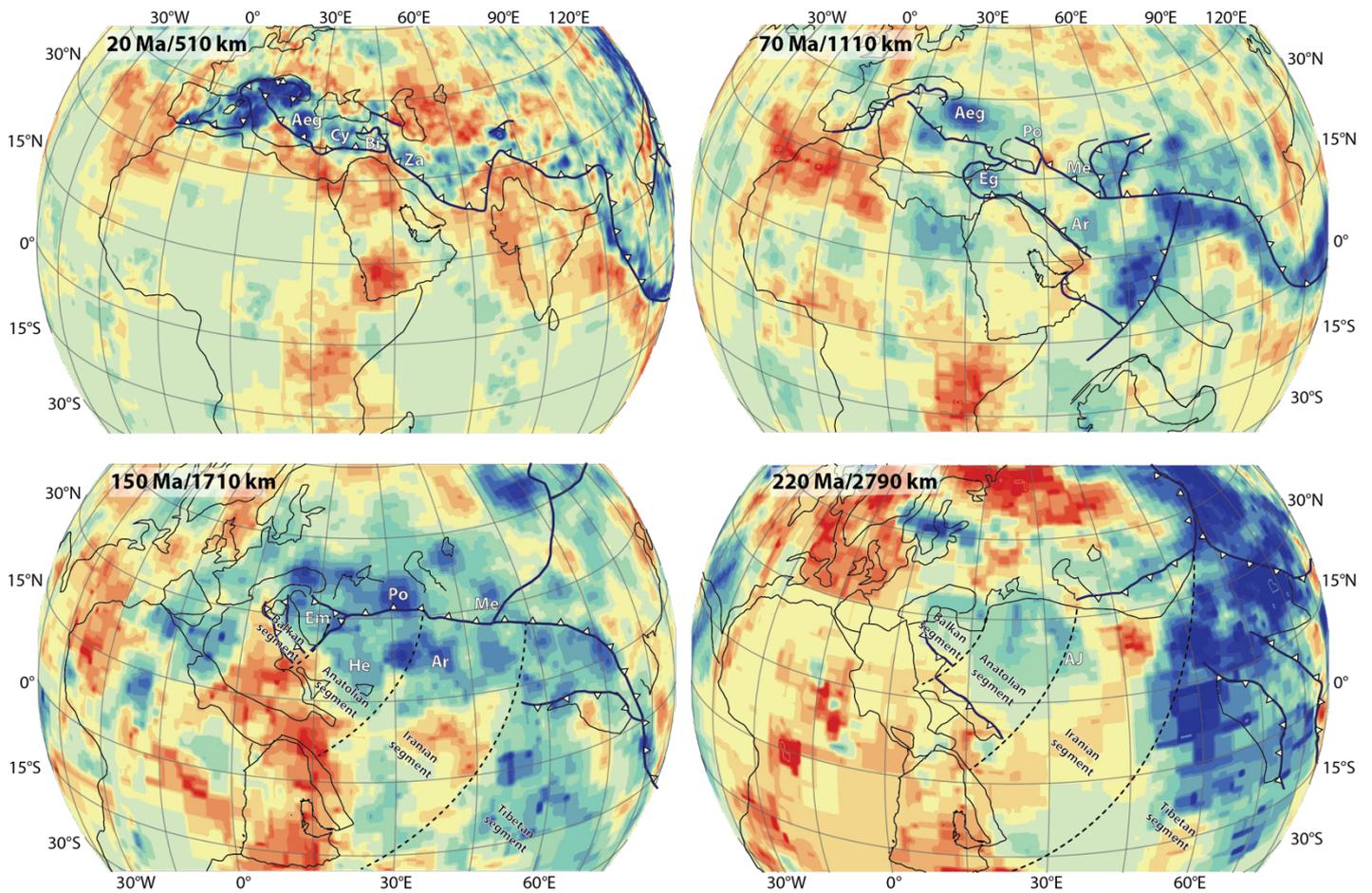
Figure 7: First-order correlation between tomography (from UU-P07 (Amaru, 2007, Hall and Spakman, 2015)) and reconstructions of continents, trenches and transforms (van Hinsbergen et al., 2026, Lom and van Hinsbergen, 2026) for the Balkan, Anatolia, Iranian and Tibetan segments. Slab sinking rates vary as a function of the absolute trench motion during subduction (Figure 5) and above and below the transition zone. The predicted locations of slabs of the Neotethyan subduction segments by the minimum-continent-motion mantle reference frame of Wagenaar et al. (2025) generally agree well with the slab patterns and edges imaged in the lower mantle and suggest minimal horizontal mantle flow in the Tethyan realm since the Mesozoic. For detailed interpretations of slabs in the Tibetan segment and below east Asia, see van der Meer

et al. (2018), Parsons et al. (2020) and Qayyum et al. (2022). The Triassic (220 Ma) prediction appears offset eastward relative to mantle structure by ~10°. See text for more explanation. Aeg = Aegean slab; AJ = Al Jawf slab; Ar = Arabia slabs; Bi = Bitlis Slab; Cy = Cyprus slab; Eg = Egypt slab; Em = Emporios slab; He = Herodotus slab; Me = Mesopotamia slab; Po = Pontides slab; Za = Zagros slab.

6. Conclusion

The tectonic history of the Eastern Mediterranean region has long been recognized to have formed due to the closure of ocean basins, collectively known as the Tethyan oceans, from the early Triassic until the present. Global correlations between plate tectonic reconstructions of subduction history, and subducted slab remnants imaged by seismic tomography have shown that slabs that formed during the closure of the Anatolian segment of the Tethyan oceans are likely still visible by tomographic imaging in the upper and especially lower mantle. In this paper, we provide the first comprehensive interpretation of lower mantle structure below the eastern Mediterranean region and Middle East, and identify, in addition to re-assessing previously described slabs, two new major slabs (Pontides, Herodotus) in the Anatolian segment. Although the Pontides and Herodotus slabs subducted at markedly different times, they are presently positioned next to each other with their bases at comparable depths. We explain this by contrasting upper-mantle subduction styles: mantle-stationary subduction of the Pontide slab promoted rapid sinking through the upper mantle and transition zone, while rollback of the Paleotethys slab resulted in a more horizontal slab geometry and therefore slower sinking. These observations suggest that globally averaged slab-sinking rates and the use of a mantle reference frame are not appropriate for such systems.

The slabs underlying the present day eastern Mediterranean and Middle East are well explained by their position of slab detachment inferred from a plate kinematic reconstruction placed in a recent minimum-continent-motion mantle reference frame, assuming only vertical sinking. Similar previous conclusions from the Tibetan segment of the Tethyan system corroborates the suggestion by this reference frame for minimal paleo-longitudinal plate motion of the Tethyan realm since the Triassic. Moreover, these correlations suggest that any ambient, bottom-up driven mantle convective flow did not lead to identifiable lateral displacements of Tethyan slabs since the Triassic relative to Eurasia, suggesting that lower mantle flow is subordinate compared to plate motion.

Acknowledgements

Data availability statement

There are no new data used for this paper. The UUP07 tomographic model is available on https://www.atlas-of-the-underworld.org/downloads/. For plate reconstruction files, see supplementary information of van Hinsbergen *et al.* (2026).

7. References

Abdelwahed, M.F., 2025. Seismic Tomography Applications in Eastern Mediterranean Region: A Review. *in Seismotectonics of the East Mediterranean-Red Sea region*, pp. 629-649, eds. Hamimi, Z., Németh, K., Fowler, A.-R., Arai, S., Peláez, J. A., Toni, M. & Sawires, R. Springer Nature.

Agard, P., Omrani, J., Jolivet, L., Whitechurch, H., Vrielynck, B., Spakman, W., Monié, P., Meyer, B. & Wortel, R., 2011. Zagros orogeny: a subduction-dominated process, *Geological Magazine,* 148**,** 692-725.

Al-Riyami, K., Robertson, A., Dixon, J. & Xenophontos, C., 2002. Origin and emplacement of the Late Cretaceous Baer–Bassit ophiolite and its metamorphic sole in NW Syria, *Lithos,* 65**,** 225-260.

Allen, M.B., Kheirkhah, M., Emami, M.H. & Jones, S.J., 2011. Right-lateral shear across Iran and kinematic change in the Arabia-Eurasia collision zone, *Geophysical Journal International,* 184**,** 555-574.

Amaru, M., 2007. *Global travel time tomography with 3-D reference models,* edn, Vol. 274, pp. Pages, Utrecht University.

Andrew, T. & Robertson, A.H.F., 2002. The Beyşehir–Hoyran–Hadim Nappes: genesis and emplacement of Mesozoic marginal and oceanic units of the northern Neotethys in southern Turkey, *Journal of the Geological Society of London,* 159**,** 529-543.

Auer, L., Boschi, L., Becker, T., Nissen-Meyer, T. & Giardini, D., 2014. Savani: A variable resolution whole-mantle model of anisotropic shear velocity variations based on multiple data sets, *Journal of Geophysical Research: Solid Earth,* 119**,** 3006-3034.

Avdeev, B. & Niemi, N.A., 2011. Rapid Pliocene exhumation of the Central Greater Caucasus constrained by low-temperature thermochronometry, *Tectonics,* 30.

Bagheri, S. & Gol, S.D., 2020. The Eastern Iranian Orocline, *Earth-Science Reviews***,** 103322.

Barrier, E. & Vrielynck, B., 2008. MEBE atlas of paleotectonic maps of the Middle East: Commission for the geological map of the worldParis.

Becker, T.W. & Boschi, L., 2002. A comparison of tomographic and geodynamic mantle models, *Geochemistry, Geophysics, Geosystems,* 3.

Becker, T.W. & Faccenna, C., 2011. Mantle conveyor beneath the Tethyan collisional belt, *Earth and Planetary Science Letters,* 310**,** 453-461.

Berberian, F. & Berberian, M., 1981. Tectono-plutonic episodes in Iran, *Zagros Hindu Kush Himalaya Geodynamic Evolution,* 3**,** 5-32.

Bijwaard, H. & Spakman, W., 1999. Tomographic evidence for a narrow whole mantle plume below Iceland, *Earth and Planetary Science Letters,* 166**,** 121-126.

Bijwaard, H., Spakman, W. & Engdahl, E.R., 1998. Closing the gap between regional and global travel time tomography, *Journal of Geophysical Research: Solid Earth,* 103**,** 30055-30078.

Biryol, C.B., Beck, S.L., Zandt, G. & Özacar, A.A., 2011. Segmented African lithosphere beneath the Anatolian region inferred from teleseismic P-wave tomography, *Geophysical Journal International,* 184**,** 1037-1057.

Boschman, L.M., van Hinsbergen, D.J.J., Kimbrough, D.L., Langereis, C.G. & Spakman, W., 2018. The dynamic history of 220 million years of subduction below Mexico: a correlation between slab geometry and overriding plate deformation based on geology, paleomagnetism, and seismic tomography, *Geochemistry, Geophysics, Geosystems,* 19**,** 4649-4672.

Boutoux, A., Briaud, A., Faccenna, C., Ballato, P., Rossetti, F. & Blanc, E., 2021. Slab folding and surface deformation of the Iran mobile belt, *Tectonics,* 40**,** e2020TC006300.

Butterworth, N.P., Talsma, A.S., Müller, R.D., Seton, M., Bunge, H.P., Schuberth, B.S.A., Shephard, G.E. & Heine, C., 2014. Geological, tomographic, kinematic and geodynamic constraints on the dynamics of sinking slabs, *Journal of Geodynamics,* 73**,** 1-13.

Cavazza, W., Cattò, S., Zattin, M., Okay, A.I. & Reiners, P., 2018. Thermochronology of the Miocene Arabia-Eurasia collision zone of southeastern Turkey, *Geosphere,* 14**,** 2277-2293.

Cawood, P.A., Kröner, A., Collins, W.J., Kusky, T.M., Mooney, W.D. & Windley, B.F., 2009. Accretionary orogens through Earth history, *Geological Society, London, Special Publications,* 318**,** 1-36.

Çelik, Ö.F., Delaloye, M. & Feraud, G., 2006. Precise 40 Ar– 39 Ar ages from the metamorphic sole rocks of the Tauride Belt Ophiolites, southern Turkey: implications for the rapid cooling history, *Geological Magazine,* 143.

Chang, S.-J., van der Lee, S., Flanagan, M.P., Bedle, H., Marone, F., Matzel, E.M., Pasyanos, M.E., Rodgers, A.J., Romanowicz, B. & Schmid, C., 2010. Joint inversion for three-dimensional S-velocity mantle structure along the Tethyan margin, *Journal of Geophysical Research,* 115.

Chen, Y.-W., Wu, J. & Goes, S., 2024. Lesser Antilles slab reconstruction reveals lateral slab transport under the Caribbean since 50 Ma, *Earth and Planetary Science Letters,* 627**,** 118561.

Chen, Y.-W., Wu, J. & Suppe, J., 2019. Southward propagation of Nazca subduction along the Andes, *Nature,* 565**,** 441.

Chiu, H.-Y., Chung, S.-L., Zarrinkoub, M.H., Mohammadi, S.S., Khatib, M.M. & Iizuka, Y., 2013. Zircon U–Pb age constraints from Iran on the magmatic evolution related to Neotethyan subduction and Zagros orogeny, *Lithos,* 162-163**,** 70-87.

Čížková, H. & Bina, C.R., 2015. Geodynamics of trench advance: Insights from a Philippine-Sea-style geometry, *Earth and Planetary Science Letters,* 430**,** 408-415.

Confal, J.M., Taymaz, T., Eken, T., Bezada, M.J. & Faccenda, M., 2025. Remnant Tethyan slab fragments beneath northern Türkiye, *Earth and Planetary Science Letters,* 664**,** 119458.

Cowgill, E., Forte, A.M., Niemi, N., Avdeev, B., Tye, A., Trexler, C., Javakhishvili, Z., Elashvili, M. & Godoladze, T., 2016. Relict basin closure and crustal shortening budgets during continental collision: An example from Caucasus sediment provenance, *Tectonics,* 35**,** 2918-2947.

De Boorder, H., Spakman, W., White, S. & Wortel, M., 1998. Late Cenozoic mineralization, orogenic collapse and slab detachment in the European Alpine Belt, *Earth and Planetary Science Letters,* 164**,** 569-575.

DeMets, C. & Merkouriev, S., 2021. Detailed reconstructions of India–Somalia Plate motion, 60 Ma to present: implications for Somalia Plate absolute motion and India–Eurasia Plate motion, *Geophysical Journal International,* 227**,** 1730-1767.

Dilek, Y., Thy, P., Hacker, B. & Grundvig, S., 1999. Structure and petrology of Tauride ophiolites and mafic dike intrusions (Turkey): Implications for the Neotethyan ocean, *Geological Society of America Bulletin,* 111**,** 1192-1216.

Dokuz, A., Aydınçakır, E., Kandemir, R., Karslı, O., Siebel, W., Derman, A.S. & Turan, M., 2017. Late Jurassic Magmatism and Stratigraphy in the Eastern Sakarya Zone, Turkey: Evidence for the Slab Breakoff of Paleotethyan Oceanic Lithosphere, *The Journal of Geology,* 125**,** 1-31.

Domeier, M., Doubrovine, P.V., Torsvik, T.H., Spakman, W. & Bull, A.L., 2016. Global correlation of lower mantle structure and past subduction, *Geophysical Research Letters,* 43**,** 4945-4953.

Faccenna, C., Becker, T.W., Auer, L., Billi, A., Boschi, L., Brun, J.P., Capitanio, F.A., Funiciello, F., Horvàth, F. & Jolivet, L., 2014. Mantle dynamics in the Mediterranean, *Reviews of Geophysics,* 52**,** 283-332.

Faccenna, C., Bellier, O., Martinod, J., Piromallo, C. & Regard, V., 2006. Slab detachment beneath eastern Anatolia: A possible cause for the formation of the North Anatolian fault, *Earth and Planetary Science Letters,* 242**,** 85-97.

Faccenna, C., Jolivet, L., Piromallo, C. & Morelli, A., 2003. Subduction and the depth of convection in the Mediterranean mantle, *Journal of Geophysical Research: Solid Earth,* 108.

Forte, A.M., Cowgill, E. & Whipple, K.X., 2014. Transition from a singly vergent to doubly vergent wedge in a young orogen: The Greater Caucasus, *Tectonics,* 33**,** 2077-2101.

French, S.W. & Romanowicz, B., 2015. Broad plumes rooted at the base of the Earth's mantle beneath major hotspots, *Nature,* 525**,** 95-99.

Fritzell, E.H., Bull, A.L. & Shephard, G.E., 2016. Closure of the Mongol–Okhotsk Ocean: Insights from seismic tomography and numerical modelling, *Earth and Planetary Science Letters,* 445**,** 1-12.

Fukao, Y., Widiyantoro, S. & Obayashi, M., 2001. Stagnant slabs in the upper and lower mantle transition region, *Reviews of Geophysics,* 39**,** 291-323.

Fuston, S. & Wu, J., 2021. Raising the Resurrection plate from an unfolded-slab plate tectonic reconstruction of northwestern North America since early Cenozoic time, *Geological Society of America Bulletin,* 133**,** 1128-1140.

Fuston, S., Wu, J. & Colli, L., 2025. Cretaceous collision reconciles western North American tectonics with deep mantle slabs. *in Jurassic–Paleogene Tectonic Evolution of the North American Cordillera*, eds. Gordon, S. M., Miller, R. B., Rusmore, M. E. & Tikoff, B. Geological Society of America Special Paper.

Goes, S., Spakman, W. & Bijwaard, H., 1999. A lower mantle source for central European volcanism, *Science,* 286**,** 1928-1931.

Göğüş, O.H., Pysklywec, R.N., Şengör, A. & Gün, E., 2017. Drip tectonics and the enigmatic uplift of the Central Anatolian Plateau, *Nature communications,* 8**,** 1538.

Govers, R. & Fichtner, A., 2016. Signature of slab fragmentation beneath Anatolia from full-waveform tomography, *Earth and Planetary Science Letters,* 450**,** 10-19.

Grand, S.P., Van der Hilst, R.D. & Widiyantoro, S., 1997. High resolution global tomography: a snapshot of convection in the Earth, *Geological Society of America Today,* 7.

Granot, R., 2016. Palaeozoic oceanic crust preserved beneath the eastern Mediterranean, *Nature Geoscience,* 9**,** 701-705.

Gürer, D., Granot, R. & van Hinsbergen, D.J.J., 2022. Plate tectonic chain reaction revealed by noise in the Cretaceous Quiet Zone, *Nature Geoscience,* 15**,** 233-239.

Gürer, D., Plunder, A., Kirst, F., Corfu, F., Schmid, S.M. & van Hinsbergen, D.J.J., 2018. A long-lived Late Cretaceous–early Eocene extensional province in Anatolia? Structural evidence from the Ivriz Detachment, southern central Turkey, *Earth and Planetary Science Letters,* 481**,** 111-124.

Gürer, D. & van Hinsbergen, D.J.J., 2019. Diachronous demise of the Neotethys Ocean as a driver for non-cylindrical orogenesis in Anatolia, *Tectonophysics,* 760**,** 95-106.

Gürer, D., van Hinsbergen, D.J.J., Matenco, L., Corfu, F. & Cascella, A., 2016. Kinematics of a former oceanic plate of the Neotethys revealed by deformation in the Ulukışla basin (Turkey), *Tectonics,* 35**,** 2385-2416.

Hafkenscheid, E., Wortel, M.J.R. & Spakman, W., 2006. Subduction history of the Tethyan region derived from seismic tomography and tectonic reconstructions, *Journal of Geophysical Research,* 111.

Hall, R. & Spakman, W., 2015. Mantle structure and tectonic history of SE Asia, *Tectonophysics,* 658**,** 14-45.

Handy, M.R., Schmid, S.M., Bousquet, R., Kissling, E. & Bernoulli, D., 2010. Reconciling plate-tectonic reconstructions of Alpine Tethys with the geological–geophysical record of spreading and subduction in the Alps, *Earth-Science Reviews,* 102**,** 121-158.

Hüsing, S.K., Zachariasse, W.-J., van Hinsbergen, D.J.J., Krijgsman, W., Inceöz, M., Harzhauser, M., Mandic, O. & Kroh, A., 2009. Oligocene–Miocene basin evolution in SE Anatolia, Turkey: constraints on the closure of the eastern Tethys gateway, *Geological Society, London, Special Publications,* 311**,** 107-132.

Inwood, J., Morris, A., Anderson, M.W. & Robertson, A.H.F., 2009. Neotethyan intraoceanic microplate rotation and variations in spreading axis orientation: Palaeomagnetic evidence from the Hatay ophiolite (southern Turkey), *Earth and Planetary Science Letters,* 280**,** 105-117.

Jagoutz, O., Royden, L., Holt, A.F. & Becker, T.W., 2015. Anomalously fast convergence of India and Eurasia caused by double subduction, *Nature Geoscience,* 8**,** 475-478.

Jolivet, L. & Brun, J.-P., 2010. Cenozoic geodynamic evolution of the Aegean, *International Journal of Earth Sciences,* 99**,** 109-138.

Jolivet, L., Faccenna, C., Agard, P., Frizon de Lamotte, D., Menant, A., Sternai, P. & Guillocheau, F., 2015. Neo-Tethys geodynamics and mantle convection: from extension to compression in Africa and a conceptual model for obduction, *Canadian journal of earth sciences,* 53**,** 1190-1204.

Kalyoncuoğlu, Ü.Y., Elitok, Ö., Dolmaz, M.N. & Anadolu, N.C., 2011. Geophysical and geological imprints of southern Neotethyan subduction between Cyprus and the Isparta Angle, SW Turkey, *Journal of Geodynamics,* 52**,** 70-82.

Kapp, P. & DeCelles, P.G., 2019. Mesozoic–Cenozoic geological evolution of the Himalayan-Tibetan orogen and working tectonic hypotheses, *American Journal of Science,* 319**,** 159-254.

Karakhanian, A.S., Trifonov, V.G., Philip, H., Avagyan, A., Hessami, K., Jamali, F., Bayraktutan, M.S., Bagdassarian, H., Arakelian, S. & Davtian, V., 2004. Active faulting and natural hazards in Armenia, eastern Turkey and northwestern Iran, *Tectonophysics,* 380**,** 189-219.

Kaymakci, N., Özçelik, Y., White, S.H. & Van Dijk, P.M., 2009. Tectono-stratigraphy of the Çankırı Basin: Late Cretaceous to early Miocene evolution of the Neotethyan Suture Zone in Turkey, *Geological Society, London, Special Publications,* 311**,** 67-106.

Keskin, M., 2003. Magma generation by slab steepening and breakoff beneath a subduction-accretion complex: An alternative model for collision-related volcanism in Eastern Anatolia, Turkey, *Geophysical Research Letters,* 30.

Koç, A., van Hinsbergen, D.J.J., Kaymakci, N. & Langereis, C.G., 2016. Late Neogene oroclinal bending in the central Taurides: A record of terminal eastward subduction in southern Turkey?, *Earth and Planetary Science Letters,* 434**,** 75-90.

Koulakov, I., 2011. High-frequency P and S velocity anomalies in the upper mantle beneath Asia from inversion of worldwide traveltime data, *Journal of Geophysical Research,* 116.

Koulakov, I., Zabelina, I., Amanatashvili, I. & Meskhia, V., 2012. Nature of orogenesis and volcanism in the Caucasus region based on results of regional tomography, *Solid Earth,* 3**,** 327-337.

Kounoudis, R., Bastow, I., Ogden, C., Goes, S., Jenkins, J., Grant, B. & Braham, C., 2020. Seismic tomographic imaging of the Eastern Mediterranean mantle: Implications for terminal-stage subduction, the uplift of Anatolia, and the development of the North Anatolian Fault, *Geochemistry, Geophysics, Geosystems,* 21**,** e2020GC009009.

Labails, C., Olivet, J.-L., Aslanian, D. & Roest, W.R., 2010. An alternative early opening scenario for the Central Atlantic Ocean, *Earth and Planetary Science Letters,* 297**,** 355-368.

Lei, J. & Zhao, D., 2007. Teleseismic evidence for a break-off subducting slab under Eastern Turkey, *Earth and Planetary Science Letters,* 257**,** 14-28.

Li, C., van der Hilst, R.D., Engdahl, E.R. & Burdick, S., 2008. A new global model for Pwave speed variations in Earth's mantle, *Geochemistry, Geophysics, Geosystems,* 9**,** n/a-n/a.

Lom, N. & van Hinsbergen, D.J.J., 2026. Reconstruction of plate tectonic evolution and orogenesis of the Central Tethysides (Iran, Afghanistan) since the Permian, *Gondwana Research,* submitted, preprint at https://doi.org/10.31223/X5N760.

Ma, Y., Dekkers, M.J., Duarte, J.C. & Kusky, T., 2025. Subduction transference drove the Mesozoic convergence of microcontinents from Gondwana to Asia, *Communications Earth & Environment,* 6**,** 442.

Maffione, M. & van Hinsbergen, D.J.J., 2018. Reconstructing plate boundaries in the Jurassic Neo-Tethys from the East and West Vardar Ophiolites (Greece, Serbia), *Tectonics*.

Maffione, M., van Hinsbergen, D.J.J., de Gelder, G.I.N.O., van der Goes, F.C. & Morris, A., 2017. Kinematics of Late Cretaceous subduction initiation in the Neo-Tethys Ocean reconstructed from ophiolites of Turkey, Cyprus, and Syria, *Journal of Geophysical Research: Solid Earth,* 122**,** 3953-3976.

Maggi, A. & Priestley, K., 2005. Surface waveform tomography of the Turkish-Iranian plateau, *Geophysical Journal International,* 160**,** 1068-1080.

McPhee, P.J., Altıner, D. & van Hinsbergen, D.J.J., 2018. First Balanced Cross Section Across the Taurides Fold-Thrust Belt: Geological Constraints on the Subduction History of the Antalya Slab in Southern Anatolia, *Tectonics,* 37**,** 3738-3759.

McPhee, P.J., Koç, A. & van Hinsbergen, D.J.J., 2022. Preparing the ground for plateau growth: Late Neogene Central Anatolian uplift in the context of orogenic and geodynamic evolution since the Cretaceous, *Tectonophysics,* 822**,** 229131.

McPhee, P.J. & van Hinsbergen, D.J.J., 2019. Tectonic reconstruction of Cyprus reveals Late Miocene continental collision between Africa and Anatolia, *Gondwana Research,* 68**,** 158-173.

McPhee, P.J., van Hinsbergen, D.J.J. & Thomson, S., 2019. Thermal history of the western Central Taurides fold-thrust belt: Implications for Cenozoic vertical motions of southern Central Anatolia, *Geosphere,* 15**,** 1927-1942.

McQuarrie, N., Stock, J.M., Verdel, C. & Wernicke, B.P., 2003. Cenozoic evolution of Neotethys and implications for the causes of plate motions, *Geophysical Research Letters,* 30**,** n/a-n/a.

Menichelli, I., De Gori, P., Funiciello, F. & Claudio, C., 2025. The two-sided continental subduction of the Adria microplate (Mediterranean), *Geology,* 53**,** 296-300.

Miller, M., Gorbatov, A. & Kennett, B., 2005. Heterogeneity within the subducting Pacific slab beneath the Izu–Bonin–Mariana arc: Evidence from tomography using 3D ray tracing inversion techniques, *Earth and Planetary Science Letters,* 235**,** 331-342.

Moghadam, H.S. & Stern, R.J., 2011. Geodynamic evolution of Upper Cretaceous Zagros ophiolites: formation of oceanic lithosphere above a nascent subduction zone, *Geological Magazine,* 148**,** 762-801.

Mohajjel, M. & Fergusson, C., 2014. Jurassic to Cenozoic tectonics of the Zagros Orogen in northwestern Iran, *International Geology Review,* 56**,** 263-287.

Moix, P., Beccaletto, L., Kozur, H.W., Hochard, C., Rosselet, F. & Stampfli, G.M., 2008. A new classification of the Turkish terranes and sutures and its implication for the paleotectonic history of the region, *Tectonophysics,* 451**,** 7-39.

Morris, A. & Anderson, M.W., 2002. Palaeomagnetic results from the Baër-Bassit ophiolite of northern Syria and their implication for fold tests in sheeted dyke terrains, *Physics and Chemistry of the Earth, Parts A/B/C,* 27**,** 1215-1222.

Mueller, M., Licht, A., Campbell, C., Ocakoğlu, F., Taylor, M., Burch, L., Ugrai, T., Kaya, M., Kurtoğlu, B. & Coster, P., 2019. Collision chronology along the İzmir-Ankara-Erzincan suture zone: Insights from the Sarıcakaya Basin, western Anatolia, *Tectonics,* 38**,** 3652-3674.

Mueller, M.A., Licht, A., Campbell, C., Ocakoğlu, F., Akşit, G.G., Métais, G., Coster, P.M., Beard, K.C. & Taylor, M.H., 2022. Sedimentary provenance from the evolving forearc-to-foreland Central Sakarya Basin, western Anatolia reveals multi-phase intercontinental collision, *Geochemistry, Geophysics, Geosystems,* 23**,** e2021GC010232.

Mumladze, T., Forte, A.M., Cowgill, E.S., Trexler, C.C., Niemi, N.A., Burak Yıkılmaz, M. & Kellogg, L.H., 2015. Subducted, detached, and torn slabs beneath the Greater Caucasus, *GeoResJ,* 5**,** 36-46.

Munteanu, I., Matenco, L., Dinu, C. & Cloetingh, S., 2011. Kinematics of back-arc inversion of the Western Black Sea Basin, *Tectonics,* 30**,** n/a-n/a.

Muttoni, G., Mattei, M., Balini, M., Zanchi, A., Gaetani, M. & Berra, F., 2009. The drift history of Iran from the Ordovician to the Triassic, *Geological Society, London, Special Publications,* 312**,** 7-29.

Nolet, G., Allen, R. & Zhao, D., 2007. Mantle plume tomography, *Chemical Geology,* 241**,** 248-263.

Obayashi, M., Yoshimitsu, J., Nolet, G., Fukao, Y., Shiobara, H., Sugioka, H., Miyamachi, H. & Gao, Y., 2013. Finite frequency whole mantle P wave tomography: Improvement of subducted slab images, *Geophysical Research Letters,* 40**,** 5652-5657.

Okay, A.I., Celal Sengor, A.M. & Görür, N., 1994. Kinematic history of the opening of the Black Sea and its effect on the surrounding regions, *Geology,* 22**,** 267-270.

Okay, A.I. & Nikishin, A.M., 2015. Tectonic evolution of the southern margin of Laurasia in the Black Sea region, *International Geology Review,* 57**,** 1051-1076.

Okay, A.I., Sunal, G., Sherlock, S., Alt, ner, D., Tüysüz, O., Kylander-Clark, A.R.C. & Aygül, M., 2013. Early Cretaceous sedimentation and orogeny on the active margin of Eurasia: Southern Central Pontides, Turkey, *Tectonics,* 32**,** 1247-1271.

Okay, A.I., Zattin, M. & Cavazza, W., 2010. Apatite fission-track data for the Miocene Arabia-Eurasia collision, *Geology,* 38**,** 35-38.

Omrani, J., Agard, P., Whitechurch, H., Benoit, M., Prouteau, G. & Jolivet, L., 2008. Arc-magmatism and subduction history beneath the Zagros Mountains, Iran: A new report of adakites and geodynamic consequences, *Lithos,* 106**,** 380-398.

Özgül, N., 1984. Stratigraphy and tectonic evolution of the Central Taurides, *Geology of the Taurus belt***,** 77-90.

Parsons, A.J., Hosseini, K., Palin, R. & Sigloch, K., 2020. Geological, geophysical and plate kinematic constraints for models of the India-Asia collision and the post-Triassic central Tethys oceans, *Earth-Science Reviews***,** 103084.

Parsons, A.J., Sigloch, K. & Hosseini, K., 2021. Australian Plate Subduction is Responsible for Northward Motion of the India-Asia Collision Zone and~ 1,000 km Lateral Migration of the Indian Slab, *Geophysical Research Letters,* 48**,** e2021GL094904.

Patriat, P. & Achache, J., 1984. India-Eurasia collision chronology has implications for crustal shortening and driving mechanism of plates, *Nature,* 311**,** 615-621.

Peng, D. & Liu, L., 2022. Quantifying slab sinking rates using global geodynamic models with data-assimilation, *Earth-Science Reviews,* 230**,** 104039.

Piromallo, C. & Morelli, A., 1997. Imaging the Mediterranean upper mantle by P-wave travel time tomography, *Annals of Geophysics,* 40.

Piromallo, C. & Morelli, A., 2003. Pwave tomography of the mantle under the Alpine-Mediterranean area, *Journal of Geophysical Research: Solid Earth,* 108.

Pokorný, J., Čížková, H. & van den Berg, A., 2021. Feedbacks between subduction dynamics and slab deformation: Combined effects of nonlinear rheology of a weak decoupling layer and phase transitions, *Physics of the Earth and Planetary Interiors,* 313**,** 106679.

Portner, D.E., Delph, J.R., Biryol, C.B., Beck, S.L., Zandt, G., Özacar, A.A., Sandvol, E. & Türkelli, N., 2018. Subduction termination through progressive slab deformation across Eastern Mediterranean subduction zones from updated P-wave tomography beneath Anatolia, *Geosphere,* 14**,** 907-925.

Pourteau, A., Scherer, E.E., Schorn, S., Bast, R., Schmidt, A. & Ebert, L., 2019. Thermal evolution of an ancient subduction interface revealed by Lu–Hf garnet geochronology, Halilbağı Complex (Anatolia), *Geoscience Frontiers,* 10**,** 127-148.

Pourteau, A., Sudo, M., Candan, O., Lanari, P., Vidal, O. & Oberhänsli, R., 2013. Neotethys closure history of Anatolia: insights from 40Ar-39Ar geochronology andP-Testimation in high-pressure metasedimentary rocks, *Journal of Metamorphic Geology,* 31**,** 585-606.

Pownall, J.M., Lister, G.S. & Spakman, W., 2017. Reconstructing subducted oceanic lithosphere by "reverse-engineering" slab geometries: The northern Philippine Sea Plate, *Tectonics,* 36**,** 1814-1834.

Qayyum, A., Lom, N., Advokaat, E.L., Spakman, W., Van Der Meer, D.G. & van Hinsbergen, D.J.J., 2022. Subduction and slab detachment under moving trenches during ongoing India-Asia convergence, *Geochemistry, Geophysics, Geosystems***,** e2022GC010336.

Rahmani, M., Motaghi, K., Ghods, A., Sobouti, F., Talebian, M., Ai, Y. & Chen, L., 2019. Deep velocity image of the north Zagros collision zone (Iran) from regional and teleseismic tomography, *Geophysical Journal International,* 219**,** 1729-1740.

Replumaz, A., Kárason, H., van der Hilst, R.D., Besse, J. & Tapponnier, P., 2004. 4-D evolution of SE Asia's mantle from geological reconstructions and seismic tomography, *Earth and Planetary Science Letters,* 221**,** 103-115.

Replumaz, A., Negredo, A.M., Guillot, S. & Villaseñor, A., 2010a. Multiple episodes of continental subduction during India/Asia convergence: Insight from seismic tomography and tectonic reconstruction, *Tectonophysics,* 483**,** 125-134.

Replumaz, A., Negredo, A.M., Villaseñor, A. & Guillot, S., 2010b. Indian continental subduction and slab break-off during Tertiary collision, *Terra Nova,* 22**,** 290-296.

Ritsema, J., Deuss, A., Van Heijst, H. & Woodhouse, J., 2011. S40RTS: a degree-40 shear-velocity model for the mantle from new Rayleigh wave dispersion, teleseismic traveltime and normal-mode splitting function measurements, *Geophysical Journal International,* 184**,** 1223-1236.

Robertson, A., 2004. Development of concepts concerning the genesis and emplacement of Tethyan ophiolites in the Eastern Mediterranean and Oman regions, *Earth-Science Reviews,* 66**,** 331-387.

Robertson, A. & Woodcock, N., 1984. The SW segment of the Antalya Complex, Turkey as a Mesozoic-Tertiary Tethyan continental margin, *Geological Society, London, Special Publications,* 17**,** 251-271.

Robertson, A.H.F., 2002. Overview of the genesis and emplacement of Mesozoic ophiolites in the Eastern Mediterranean Tethyan region, *Lithos,* 65**,** 1-67.

Robertson, A.H.F., Parlak, O. & Ustaomer, T., 2012. Overview of the Palaeozoic-Neogene evolution of Neotethys in the Eastern Mediterranean region (southern Turkey, Cyprus, Syria), *Petroleum Geoscience,* 18**,** 381-404.

Schellart, W.P., 2005. Influence of the subducting plate velocity on the geometry of the slab and migration of the subduction hinge, *Earth and Planetary Science Letters,* 231**,** 197-219.

Schmid, S.M., Bernoulli, D., Fügenschuh, B., Georgiev, N., Kounov, A., Matenco, L., Oberhänsli, R., Pleuger, J., Schefer, S., Schuster, R., Tomljenović, B., Ustaszewski, K. & van Hinsbergen, D.J.J., 2020. Tectonic units of the Alpine collision zone between Eastern Alps and Western Turkey, *Gondwana Research,* 78**,** 308-374.

Şengör, A.C., 1979. Mid-Mesozoic closure of Permo–Triassic Tethys and its implications, *Nature,* 279**,** 590-593.

Şengör, A.C., Altıner, D., Zabcı, C., Sunal, G., Lom, N., Aylan, E. & Öner, T., 2023. On the nature of the Cimmerian Continent, *Earth-Science Reviews,* 247**,** 104520.

Şengör, A.M.C., 1984. The Cimmeride orogenic system and the tectonics of Eurasia, *Geological Society of America Special Paper,* 195**,** 82.

Şengör, A.M.C., 1990. Plate tectonics and orogenic research after 25 years: A Tethyan perspective, *Earth-Science Reviews,* 27**,** 1-201.

Şengör, A.M.C., Özeren, M., Genç, T. & Zor, E., 2003. East Anatolian High Plateau as a mantle-supported, north-south shortened domal structure, *Geophysical Research Letters,* 30**,** 8050.

Şengör, A.M.C. & Yilmaz, Y., 1981. Tethyan evolution of Turkey: A plate tectonic approach, *Tectonophysics,* 75**,** 181-241.

Sharples, W., Jadamec, M., Moresi, L.-N. & Capitanio, F.A., 2014. Overriding plate controls on subduction evolution, *Journal of Geophysical Research: Solid Earth,* 119**,** 6684-6704.

Sigloch, K. & Mihalynuk, M.G., 2013. Intra-oceanic subduction shaped the assembly of Cordilleran North America, *Nature,* 496**,** 50-56.

Spakman, W., 1986. Subduction beneath Eurasia in connection with the Mesozoic Tethys, *Netherlands Journal of Geosciences***,** 145-153.

Spakman, W., Chertova, M.V., van den Berg, A. & van Hinsbergen, D.J.J., 2018. Puzzling features of western Mediterranean tectonics explained by slab dragging, *Nature Geoscience,* 11**,** 211-216.

Spakman, W., van der Lee, S. & van der Hilst, R., 1993. Travel-time tomography of the European-Mediterranean mantle down to 1400 km, *Physics of the Earth and Planetary Interiors,* 79**,** 3-74.

Spakman, W., Wortel, M. & Vlaar, N., 1988. The Hellenic subduction zone: a tomographic image and its geodynamic implications, *Geophysical research letters,* 15**,** 60-63.

Spakman, W. & Wortel, R., 2004. A Tomographic View on Western Mediterranean Geodynamics. *in The TRANSMED Atlas. The Mediterranean Region from Crust to Mantle: Geological and Geophysical Framework of the Mediterranean and the Surrounding Areas*, pp. 31-52, eds. Cavazza, W., Roure, F., Spakman, W., Stampfli, G. M. & Ziegler, P. A. Springer Berlin Heidelberg, Berlin, Heidelberg.

Speranza, F., Minelli, L., Pignatelli, A. & Chiappini, M., 2012. The Ionian Sea: The oldest in situ ocean fragment of the world?, *Journal of Geophysical Research: Solid Earth,* 117**,** n/a-n/a.

Stampfli, G.M. & Borel, G., 2002. A plate tectonic model for the Paleozoic and Mesozoic constrained by dynamic plate boundaries and restored synthetic oceanic isochrons, *Earth and Planetary Science Letters,* 196**,** 17-33.

Stöcklin, J., 1974. Possible ancient continental margins in Iran. *in The geology of continental margins*, pp. 873-887Springer.

Tapponnier, P., Peltzer, G. & Armijo, R., 1986. On the mechanics of the collision between India and Asia, *Geological Society, London, Special Publications,* 19**,** 113-157.

Tekin, U.K. & Göncüoglu, M.C., 2007. Discovery of the oldest (Upper Ladinian to Middle Carnian) radiolarian assemblages from the Bornova flysch zone in western Turkey: implications for the evolution of the Neotethyan Izmir-Ankara ocean, *Ofioliti,* 32**,** 131-150.

Tekin, U.K., Göncüoğlu, M.C. & Turhan, N., 2002. First evidence of Late Carnian radiolarians from the Izmir–Ankara suture complex, central Sakarya, Turkey: implications for the opening age of the Izmir–Ankara branch of Neo-Tethys, *Geobios,* 35**,** 127-135.

Topuz, G., Candan, O., Zack, T. & Yılmaz, A., 2017. East Anatolian plateau constructed over a continental basement: No evidence for the East Anatolian accretionary complex, *Geology,* 45**,** 791-794.

Torsvik, T.H., Rousse, S., Labails, C. & Smethurst, M.A., 2009. A new scheme for the opening of the South Atlantic Ocean and the dissection of an Aptian salt basin, *Geophysical Journal International,* 177**,** 1315-1333.

Toyokuni, G. & Zhao, D., 2025. Whole-mantle tomography beneath eastern Mediterranean and adjacent regions, *Geophysical Journal International,* 241**,** 1155-1172.

Tremblay, A., Meshi, A., Deschamps, T., Goulet, F. & Goulet, N., 2015. The Vardar zone as a suture for the Mirdita ophiolites, Albania: Constraints from the structural analysis of the Korabi-Pelagonia zone, *Tectonics,* 34**,** 352-375.

Ustaömer, T. & Robertson, A.H., 1999. Geochemical evidence used to test alternative plate tectonic models for pre-Upper Jurassic (Palaeotethyan) units in the Central Pontides, N Turkey, *Geological Journal,* 34**,** 25-53.

Ustaömer, T.m. & Robertson, A.H.F., 2010. Late Palaeozoic-Early Cenozoic tectonic development of the Eastern Pontides (Artvin area), Turkey: stages of closure of Tethys along the southern margin of Eurasia, *Geological Society, London, Special Publications,* 340**,** 281-327.

Ustaszewski, K., Kounov, A., Schmid, S.M., Schaltegger, U., Krenn, E., Frank, W. & Fügenschuh, B., 2010. Evolution of the Adria-Europe plate boundary in the northern Dinarides: From continent-continent collision to back-arc extension, *Tectonics,* 29**,** n/a-n/a.

van der Boon, A., van Hinsbergen, D.J.J., Rezaeian, M., Gürer, D., Honarmand, M., Pastor-Galán, D., Krijgsman, W. & Langereis, C.G., 2018. Quantifying Arabia–Eurasia convergence accommodated in the Greater Caucasus by paleomagnetic reconstruction, *Earth and Planetary Science Letters,* 482**,** 454-469.

Van der Hilst, R., De Hoop, M., Wang, P., Shim, S.-H., Ma, P. & Tenorio, L., 2007. Seismostratigraphy and thermal structure of Earth's core-mantle boundary region, *science,* 315**,** 1813-1817.

van der Meer, D.G., Spakman, W., van Hinsbergen, D.J.J., Amaru, M.L. & Torsvik, T.H., 2010. Towards absolute plate motions constrained by lower-mantle slab remnants, *Nature Geoscience,* 3**,** 36-40.

van der Meer, D.G., van Hinsbergen, D.J.J. & Spakman, W., 2018. Atlas of the underworld: Slab remnants in the mantle, their sinking history, and a new outlook on lower mantle viscosity, *Tectonophysics,* 723**,** 309-448.

Van der Voo, R., Spakman, W. & Bijwaard, H., 1999a. Mesozoic subducted slabs under Siberia, *Nature,* 397**,** 246-249.

Van der Voo, R., Spakman, W. & Bijwaard, H., 1999b. Tethyan subducted slabs under India, *Earth and Planetary Science Letters,* 171**,** 7-20.

van der Wiel, E., Pokorný, J., Čížková, H., Spakman, W., van den Berg, A.P. & van Hinsbergen, D.J., 2024a. Slab buckling as a driver for rapid oscillations in Indian plate motion and subduction rate, *Communications Earth & Environment,* 5**,** 316.

van der Wiel, E., van Hinsbergen, D.J.J., Thieulot, C. & Spakman, W., 2024b. Linking rates of slab sinking to long-term lower mantle flow and mixing, *Earth and Planetary Science Letters,* 625**,** 118471.

van Hinsbergen, D.J.J., Gürer, D., Koç, A. & Lom, N., 2024. Shortening and extrusion in the East Anatolian Plateau: How was Neogene Arabia-Eurasia convergence tectonically accommodated?, *Earth and Planetary Science Letters,* 641**,** 118827.

van Hinsbergen, D.J.J., Hafkenscheid, E., Spakman, W., Meulenkamp, J.E. & Wortel, R., 2005. Nappe stacking resulting from subduction of oceanic and continental lithosphere below Greece, *Geology,* 33.

van Hinsbergen, D.J.J., Kaymakci, N., Spakman, W. & Torsvik, T.H., 2010. Reconciling the geological history of western Turkey with plate circuits and mantle tomography, *Earth and Planetary Science Letters,* 297**,** 674-686.

van Hinsbergen, D.J.J., Lamont, T.N. & Guilmette, C., 2025. Lithospheric unzipping explaining hot orogenesis during continental subduction, *Tectonics,* 44**,** e2025TC008993.

van Hinsbergen, D.J.J., Lippert, P.C., Dupont-Nivet, G., McQuarrie, N., Doubrovine, P.V., Spakman, W. & Torsvik, T.H., 2012. Greater India Basin hypothesis and a two-stage Cenozoic collision between India and Asia, *Proc Natl Acad Sci U S A,* 109**,** 7659-7664.

van Hinsbergen, D.J.J., Lippert, P.C., Li, S., Huang, W., Advokaat, E.L. & Spakman, W., 2019. Reconstructing Greater India: Paleogeographic, kinematic, and geodynamic perspectives, *Tectonophysics,* 760**,** 69-94.

van Hinsbergen, D.J.J., Maffione, M., Plunder, A., Kaymakci, N., Ganerød, M., Hendriks, B.W.H., Corfu, F., Gürer, D., de Gelder, G.I.N.O., Peters, K., McPhee, P.J., Brouwer, F.M., Advokaat, E.L. & Vissers, R.L.M., 2016. Tectonic evolution and paleogeography of the Kırşehir Block and the Central Anatolian Ophiolites, Turkey, *Tectonics,* 35**,** 983-1014.

van Hinsbergen, D.J.J. & Schmid, S.M., 2012. Map view restoration of Aegean-West Anatolian accretion and extension since the Eocene, *Tectonics,* 31**,** doi: 10.1029/2012tc003132.

van Hinsbergen, D.J.J. & Schouten, T.L.A., 2021. Deciphering paleogeography from orogenic architecture: constructing orogens in a future supercontinent as thought experiment, *American Journal of Science,* 321**,** 955-1031.

van Hinsbergen, D.J.J., Steinberger, B., Doubrovine, P.V. & Gassmöller, R., 2011. Acceleration and deceleration of India-Asia convergence since the Cretaceous: Roles of mantle plumes and continental collision, *Journal of Geophysical Research,* 116.

van Hinsbergen, D.J.J., Steinberger, B., Guilmette, C., Maffione, M., Gürer, D., Peters, K., Plunder, A., McPhee, P.J., Gaina, C., Advokaat, E.L., Vissers, R.L.M. & Spakman, W., 2021. A record of plume-induced plate rotation triggering subduction initiation, *Nature Geoscience,* 14**,** 626-630.

van Hinsbergen, D.J.J., Torsvik, T., Schmid, S.M., Matenco, L., Maffione, M., Vissers, R.L.M., Gürer, D. & Spakman, W., 2020. Orogenic architecture of the Mediterranean region and kinematic reconstruction of its tectonic evolution since the Triassic, *Gondwana Research,* 81**,** 79-229.

van Hinsbergen, D.J.J., Vaes, B., Boschman, L.M., Lom, N., van de Lagemaat, S.H.A., Advokaat, E.L., de Baar, S., Paridaens, J. & Jarochowska, E., 2026. Paleolatitude.org 3.0: a calculator for paleoclimate and paleobiology studies based on a new global paleogeography model, *PLoS One,* submitted, preprintat doi: 10.31223/X5XJ22.

Veisi, M., Sobouti, F., Chevrot, S., Abbasi, M. & Shabanian, E., 2021. Upper mantle structure under the Zagros collision zone; insights from 3D teleseismic P-wave tomography, *Tectonophysics,* 819**,** 229106.

Wagenaar, S.D.M., Vaes, B. & van Hinsbergen, D.J.J., 2025. Towards reconstructing mantle convection using a minimum-continent-motion mantle reference frame *Journal of Geophysical Research,* 130**,** e2024JB030430.

Wan, B., Wu, F., Chen, L., Zhao, L., Liang, X., Xiao, W. & Zhu, R., 2019. Cyclical one-way continental rupture-drift in the Tethyan evolution: Subduction-driven plate tectonics, *Science China Earth Sciences,* 62**,** 2005–2016.

Wang, Z., Hu, J., Bao, X., Yu, C., Yang, Y. & Chen, X., 2023. Global seismic tomography reveals remnants of subducted Tethyan oceanic slabs in the deep mantle, *Science China Earth Sciences,* 66**,** 2751-2769.

Whitney, D.L., Delph, J.R., Thomson, S.N., Beck, S.L., Brocard, G.Y., Cosca, M.A., Darin, M.H., Kaymakcı, N., Meijers, M.J. & Okay, A.I., 2023. Breaking plates: Creation of the East Anatolian fault, the Anatolian plate, and a tectonic escape system, *Geology,* 51**,** 673-677.

Whitney, D.L. & Hamilton, M.A., 2004. Timing of high-grade metamorphism in central Turkey and the assembly of Anatolia, *Journal of the Geological Society,* 161**,** 823-828.

Whitney, D.L., Teyssier, C., Fayon, A.K., Hamilton, M.A. & Heizler, M., 2003. Tectonic controls on metamorphism, partial melting, and intrusion: timing and duration of regional metamorphism and magmatism in the Niğde Massif, Turkey, *Tectonophysics,* 376**,** 37-60.

Wilmsen, M., Fürsich, F.T., Seyed-Emami, K., Majidifard, M.R. & Taheri, J., 2009. The Cimmerian Orogeny in northern Iran: Tectono-stratigraphic evidence from the foreland, *Terra Nova,* 21**,** 211-218.

Wortel, M.J.R. & Spakman, W., 2000. Subduction and slab detachment in the Mediterranean-Carpathian region, *Science,* 290**,** 1910-1917.

Wu, J., Suppe, J., Lu, R. & Kanda, R., 2016. Philippine Sea and East Asian plate tectonics since 52 Ma constrained by new subducted slab reconstruction methods, *Journal of Geophysical Research: Solid Earth,* 121**,** 4670-4741.

Yin, A. & Harrison, T.M., 2000. Geologic evolution of the Himalayan-Tibetan orogen, *Annual Review of Earth and Planetary Sciences,* 28**,** 211-280.

Zahirovic, S., Matthews, K.J., Flament, N., Müller, R.D., Hill, K.C., Seton, M. & Gurnis, M., 2016. Tectonic evolution and deep mantle structure of the eastern Tethys since the latest Jurassic, *Earth-Science Reviews,* 162**,** 293-337.

Zanchi, A., Zanchetta, S., Berra, F., Mattei, M., Garzanti, E., Molyneux, S., Nawab, A. & Sabouri, J., 2009. The Eo-Cimmerian (Late? Triassic) orogeny in North Iran.

Zhang, H., Wang, F., Myhill, R. & Guo, H., 2019. Slab morphology and deformation beneath Izu-Bonin, *Nature communications,* 10**,** 1310.

Zhu, H., Bozdağ, E., Peter, D. & Tromp, J., 2012. Structure of the European upper mantle revealed by adjoint tomography, *Nature Geoscience,* 5**,** 493-498.

Zor, E., 2008. Tomographic evidence of slab detachment beneath eastern Turkey and the Caucasus, *Geophysical Journal International,* 175**,** 1273-1282.